AN ABSTRACT OF THE THESIS OF

Sheldon J. Helms for the degree of Master of Science in Electrical and Computer Engineering presented on September 3, 1999. Title: A Simple RLS-POCS Solution for Reduced Complexity ADSL Impulse Shortening.

Redacted for Privacy

Abstract approved: _____

Virginia L. Stonick

Recently, with the realization of the World Wide Web, the tremendous need for high-speed data communications has grown. Several access techniques have been proposed which utilize the existing copper twisted pair cabling. Of these, the xDSL family, particularly ADSL and VDSL, have shown great promise in providing broadband or near-broadband access through the common telephone lines. A critical component of the ADSL and VDSL systems is the guard band needed to eliminate the interference caused by the previously transmitted blocks. This guard band must come in the form of redundant samples at the start of every transmit block, and be at least as long as the channel impulse response. Since the required guard band length is much greater than the length of the actual transmitted samples, techniques to shorten the channel impulse response must be considered. In this thesis, a new algorithm based on the RLS error minimization and POCS optimization techniques will be applied to the channel impulse-shortening problem

in an ADSL environment. As will be shown, the proposed algorithm will provide a much better solution with a minimal increase in complexity as compared to the existing LMS techniques.

A Simple RLS-POCS Solution for Reduced Complexity ADSL Impulse Shortening

by

Sheldon J. Helms

A THESIS

submitted to

Oregon State University

in partial fulfillment of
the requirements for the
degree of

Master of Science

Completed September 3, 1999
Commencement June 2000

Master of Science thesis of Sheldon J. Helms presented on September 3, 1999

APPROVED:

Redacted for Privacy

Major Professor, representing Electrical and Computer Engineering

Redacted for Privacy

Chair of the Department of Electrical & Computer Engineering

Redacted for Privacy

Dean of the Graduate School

I understand that my thesis will become part of the permanent collection of Oregon State University libraries. My signature below authorizes release of my thesis to any reader upon request.

Redacted for Privacy

Sheldon J. Helms, Author

TABLE OF CONTENTS

TABLE OF CONTENTS (Continued)

LIST OF FIGURES

A SIMPLE RLS-POCS SOLUTION FOR REDUCED COMPLEXITY ADSL IMPULSE SHORTENING

1. INTRODUCTION

Over 100 years ago, Alexander Graham Bell revolutionized communication with the advent of the telephone. Today more than 700 million subscribers are connected to the phone network utilizing the copper twisted pair cables of Bell's first invention. Until recently, the 3.4 kHz voice channel was sufficient to accomplish the majority of communication tasks. With the realization of the World Wide Web, the tremendous need for high bit rates to transfer text, sound, images, and video has grown. This need for speed has required a new look at the common twisted pair cabling, and the possible additional bandwidth it can provide, most of which has lain dormant for close to a century.

New access techniques have been emerging which utilize the large fraction of unused bandwidth available on the twisted pair cables. Asymmetric digital subscriber line (ADSL) is an access technique that can provide close to 9 Mb/s access, while its successor very-high bit rate digital subscriber line (VDSL) can provide up to 52 Mb/s access. These techniques have made the idea of on-demand and real-time video almost a realization for the millions of Internet surfers using the existing copper lines already connected to their homes. Further, ADSL and VDSL not only provide high-speed data transmission, but also allows simultaneous full use of standard voice phone services through the public switched telephone network (PSTN).

Use of the existing copper telephone lines at speeds above that required to carry plain old telephone services (POTS) requires use of higher frequency portions of channel bandwidth where additional transmission impairments occur including signal attenuation, crosstalk, and signal reflections. As a result, different equalization techniques for different frequency bands are necessary. To help combat these effects, a multitone modulation scheme called Discrete Multitone Modulation (DMT) was introduced and chosen as the standardized method for ADSL transmission.

DMT uses the efficient fast-Fourier transform (FFT), which is both a well-understood and easily implementable operation with today's digital signal processors, to modulate and demodulate the signal for transmission. Essentially the FFT divides the channel into sub-bands, where the data rate in each channel can be adaptively adjusted to carry the maximum amount of data for that channel. This is in contrast to the other method of ADSL transmission, called carrierless amplitude/phase modulation (CAP), which uses a variation of quadrature amplitude modulation (QAM) to create constellations of amplitude/phase pairs. In CAP the data rate can only be adjusted by adding more constellation points, or by increasing the transmission rate of the amplitude/phase pairs depending on the impairments of all bands in the entire channel. Due to the severe channel impairments of the ADSL environment, CAP is confined to working on very short loop lengths, where the channel impairments are less severe.

The challenges in using the DMT for ADSL transmission is to provide a channel output symbol which is independent of previous symbol transmissions and also appears to have been circularly convolved with the input. By placing a guard

period, which is as long as the discrete channel memory, at the front of every transmitted symbol we can thus ensure independence of successive block transmissions. If this guard period consists of the last υ samples of the transmit block, where υ is the length of the channel memory, then the channel output will appear to have been circularly convolved with the input which lends itself readily to the use of the FFT to demodulate the signal. The υ repeated samples are then known as the cyclic prefix and satisfy the need for both a circular channel and independent block transmissions.

In ADSL environments the channel memory can be quite long, and an appreciable information rate reduction will be incurred by the appending of redundant information samples to the start of every transmitted symbol. In other words, for the given transmission bit rate, the ratio of information to overhead bits is decreased. Thus to reduce the necessary cyclic prefix length, a partial channel equalizer is incorporated into the DMT design to reduce the effective length of the channel, and thus the required cyclic prefix length. The goal of this thesis is to provide a computationally efficient solution to the ADSL channel impulse response-shortening problem.

The objective of this thesis is to propose an alternative to the least-mean-squares (LMS) adaptation algorithm in [1,2] and the non-recursive techniques found in [3,4,9]. Since the techniques found in [3,4,9] are not adaptive, these methods will not be pursued in this thesis. The LMS algorithm used in [1,2] is known to exhibit slow convergence and a high level of residual error upon convergence, as verified in [4]. In ADSL environments the slow convergence thus causes a longer training period, and

the residual error will result in more errors at the receiver, thus requiring more error correction codes or more sophisticated channel equalization to obtain equivalent performance.

In this thesis a new algorithm will be proposed using the recursive least squares (RLS) optimization scheme in conjunction with the projections onto convex sets (POCS) optimization techniques. It will be shown that the new algorithm can provide faster convergence and less residual error upon convergence than the traditional LMS, and provide this with a minimal amount of complexity increase. The RLS optimization scheme is known to provide a much faster convergence time than the LMS algorithm, while also providing much lower residual error. Also as will be seen, the channel-shortening problem involves the simultaneous optimization of two parameters, which naturally led to the formulation of the convex sets for which the POCS method could be used and thus provide a solution that is consistent with both parameters, easily allowing the dual optimization.

The rest of this paper will be organized as follows. In section 2 the DMT system will be defined. This will include the DMT transceiver and how this system fits into the ADSL access technology. The first part of section 3 will then define and state the general DMT equalization problem for which the new RLS-POCS optimization algorithm is developed in section 4. In section 5 the simulation results using the new algorithm will be presented and compared to the optimum solution derived in section 3. Finally section 6 provides concluding remarks and directions for future research.

2. DISCRETE MULTITONE SYSTEM DESCRIPTION

Discrete Multitone (DMT) is a modulation technique that uses the computationally efficient fast Fourier Transform (FFT) to divide a channel into a set of parallel independent subchannels. The DMT system can maximize performance for any channel by adaptively selecting the number of bits allocated to each of the independent subchannels, and thus provide the highest bit-rate possible for the particular channel given measured channel transmission impairments based on SNR measurements. This method provides the highest data-rate possible while also minimizing the errors at the receiver. The equalization method presented in this thesis provides channel impulse response shortening for DMT systems.

2.1 Discrete Multitone Transmission (DMT) Concept

The basic concept behind the DMT system is illustrated in Figure 2.1, where a twisted pair channel spectrum is shown at the left, assuming an equal number of bits-per-channel throughout the frequency band of interest. Note that the channel power spectral density (PSD) $|H(f)|^2$ is not flat, with attenuation at both high and low frequencies. If a single wideband signal were to be transmitted, the bit rate would be limited by the maximum attenuation across the entire band, or the minimum signal-to-noise ratio (SNR). Instead by partitioning the transmit spectrum into narrow bands,

each individual channel can then be loaded with the information to be transmitted, and thus provide the maximum data rate available for each channel, given the channel SNR and Shannon's channel capacity theorem. This is accomplished by transmitting at higher bit rates in subchannels with high SNR (low attenuation for fixed noise power), while poor subchannels, or those with high attenuation, receive little or no information.

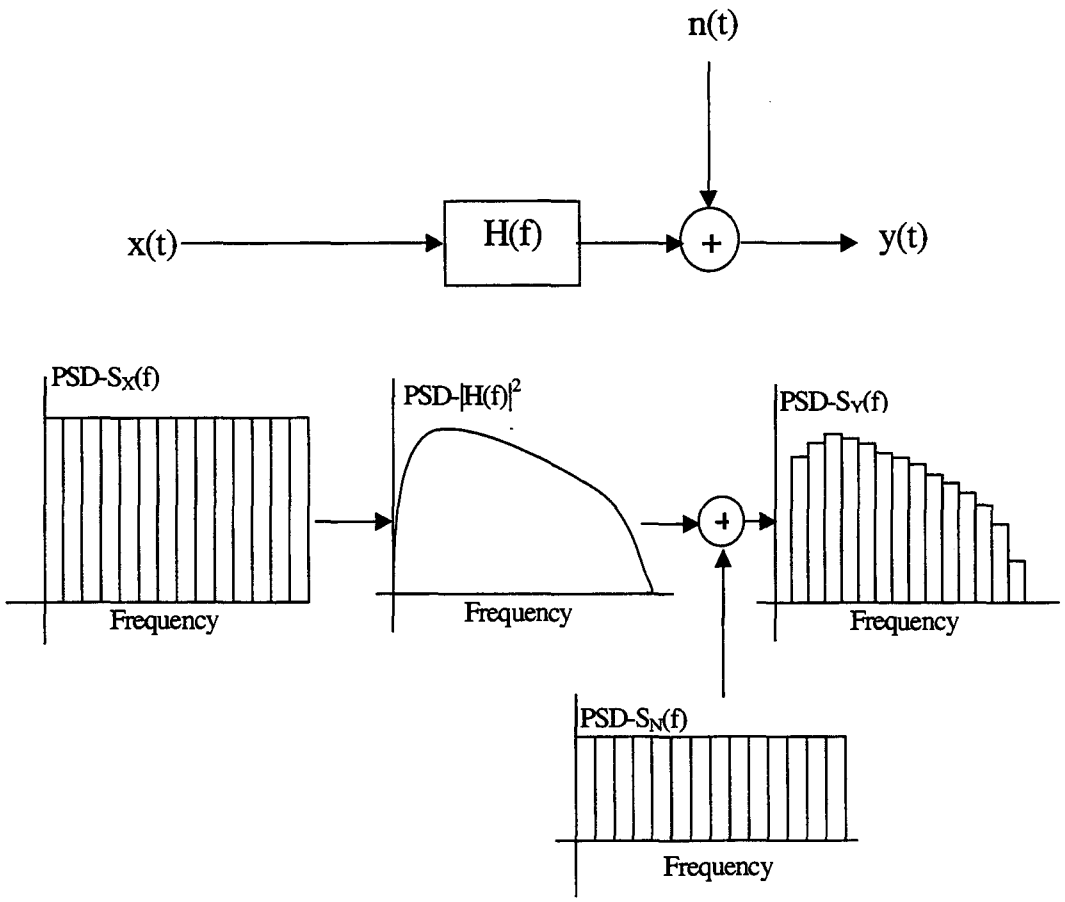

Figure 2.1 Basic Multitone Concept

2.2 Discrete Multitone Transmission (DMT) via Fast Fourier Transform (FFT)

To prevent inter-block interference (IBI) in ADSL transmission, each transmitted sequence must contain a guard band. The guard band is simply samples at the start of every transmit block which can be discarded at the receiver. If this guard band is at least as long as the channel impulse-response, then the interference from the previously transmitted sequence will be absorbed in the guard band, and the received samples corresponding to the guard band can be thrown out. This method allows successive block transmissions to be independent of one another.

A further restriction, imposed by the use of the FFT to demodulate the received signal, is for the channel output to appear as though it has been circularly convolved with the input. To necessitate this, a cyclic prefix is added to each sequence of data (symbol) samples to be transmitted over the channel. The cyclic prefix consists of the last υ input samples repeated at the beginning of the N length block, as seen in Figure 2.2. Note that the cyclic prefix is thus used as the guard band, serving a dual role.

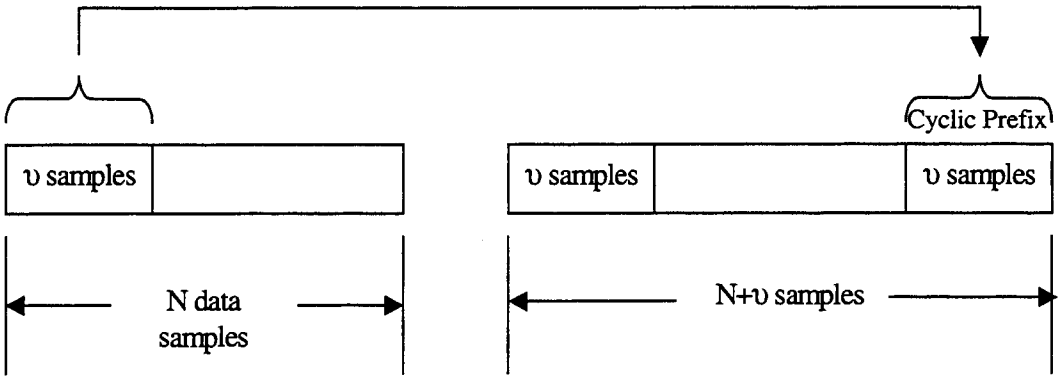

Figure 2.2 Cyclic Prefix Insertion

At the receiver, only the N samples are processed, and the υ added samples are dropped. Now, the N-length block appears to have been circularly convolved with the channel and the received sequence is IBI free and independent of adjacent block transmissions.

When the cyclic prefix is used, the channel description matrix, H_{cir}, becomes what is called a square "circulant" matrix. Circulant matrices have the property that they can be decomposed as

$$H_{cir} = Q^* \Lambda Q, \tag{2.1}$$

where Q is a matrix corresponding to the discrete Fourier transform (DFT) in which the klth element starting from the top left at k=0, l=0 is [18]

$$Q_{kl} = e^{-j\left(\frac{2\pi}{N}\right)kl}. \tag{2.2}$$

The matrix Q^* is the matrix corresponding to the inverse discrete Fourier transform (IDFT) in which the klth element starting from the top left at k=0, l=0 is

$$Q_{kl}^{*} = \frac{1}{N} e^{j\left(\frac{2\pi}{N}\right)kl}.$$

The matrix Λ is a diagonal matrix containing the N FFT values of the sequence h_k. The matrices Q and Q^* are known as the demodulation and modulation matrices respectively. As such, the transmit symbol can be mathematically represented as

$$x = Q^{*}\hat{X}, \tag{2.3}$$

where $\hat{X}$ is the vector of QAM encoded signals ordered by the Hermitian symmetry condition,

$$\begin{aligned} \hat{X}(0) &= \Re\{X(0)\} \qquad \hat{X}\left(\frac{N}{2}\right) = \Im\{X(0)\} \\ \hat{X}(k) &= X(k) \quad 1 \le k \le \frac{N}{2} - 1 \\ \hat{X}(N-k) &= X^{*}(k) \quad 1 \le k \le \frac{N}{2} - 1 \end{aligned},$$

where the symbol $\Re$ denotes the real part of the signal, $\Im$ is the imaginary, and $X^*(k)$ is the complex conjugate.

The υ last samples are then added to the output time-domain vector as a prefix yielding $\boldsymbol{x}_{cp}$ as,

$$\boldsymbol{x}_{cp} = \left[x_{N-\upsilon} \cdots x_{N-1}\, x_0\, x_1 \cdots x_{N-1}\right]^T$$

where υ is the length of the channel and N is the length of the input data vector to be explained in section 2.3. Thus the channel output can then be written as

$$\boldsymbol{y}_{cp} = H\boldsymbol{x}_{cp} + \boldsymbol{n}$$

where $\boldsymbol{n}$ is the additive white Gaussian noise vector, and H is the channel description linear convolution matrix,

$$H = \begin{bmatrix} h_\upsilon & \cdots & \cdots & \cdots & h_0 & 0 & \cdots & \cdots & 0 \\ 0 & h_\upsilon & \cdots & \cdots & \cdots & h_0 & 0 & \cdots & 0 \\ \vdots & & \ddots & & & & \ddots & & \\ 0 & \cdots & \cdots & 0 & h_\upsilon & \cdots & \cdots & \cdots & h_0 \\ \vdots & & & \ddots & & \ddots & & & \\ 0 & \cdots & \cdots & 0 & \cdots & \cdots & 0 & h_\upsilon & \end{bmatrix}.$$

Thus resulting in the output,

$$\begin{bmatrix} y_{-\upsilon} \\ \vdots \\ y_{-1} \\ y_0 \\ y_1 \\ \vdots \\ y_{N-1} \end{bmatrix} = \begin{bmatrix} h_\upsilon & \cdots & \cdots & \cdots & h_0 & 0 & \cdots & \cdots & 0 \\ 0 & h_\upsilon & \cdots & \cdots & \cdots & h_0 & 0 & \cdots & 0 \\ \vdots & & \ddots & & & & \ddots & & \\ 0 & \cdots & \cdots & 0 & h_\upsilon & \cdots & \cdots & \cdots & h_0 \\ \vdots & & & \ddots & & \ddots & & & \\ 0 & \cdots & \cdots & 0 & \cdots & \cdots & 0 & h_\upsilon & \end{bmatrix} \begin{bmatrix} *_{-\upsilon+1} \\ \vdots \\ *_{-1} \\ x_{N-\upsilon} \\ \vdots \\ x_{N-1} \\ x_0 \\ \vdots \\ x_{N-1} \end{bmatrix} + \begin{bmatrix} n_{-\upsilon} \\ \vdots \\ n_{-1} \\ n_0 \\ n_1 \\ \vdots \\ n_{N-1} \end{bmatrix},$$

where * is the $(-\upsilon+1)$ unknown samples from the previously transmitted frame. Then if the $y_{-\upsilon}$ through y_{-1} samples are discarded, which represent the samples corresponding to the cyclic prefix and contain the IBI, then the samples y_0 through y_{N-1} will represent the output from a circular channel. The circular channel description matrix can then be written as

$$H_{cir} = \begin{bmatrix} h_0 & 0 & \cdots\cdots & 0 & h_\upsilon & \cdots & h_1 \\ h_1 & h_0 & 0 & \cdots\cdots & 0 & h_\upsilon & \cdots h_2 \\ & & \ddots & & & \ddots & \\ h_{\upsilon-1} & \cdots & h_0 & 0 & \cdots & \cdots 0 & h_\upsilon \\ 0 & h_\upsilon & \cdots & h_0 & 0 & \cdots\cdots & 0 \\ \vdots & & \ddots & & \ddots & & \\ 0 & \cdots & 0 & \cdots & 0 & h_\upsilon & \cdots h_0 \end{bmatrix},$$

which implements circular convolution on the input symbols [4]. Thus the channel output can then be rewritten in terms of the circular channel, assuming the cyclic prefix has been stripped from the beginning, as

$$\boldsymbol{y} = H_{cir}\boldsymbol{x} + \boldsymbol{n}$$

where $\boldsymbol{x}$ is as defined in (2.3). Thus using (2.3) the channel output can be written

$$\boldsymbol{y} = H_{cir}Q^{*}\hat{X} + \boldsymbol{n}.$$

Then using (2.2) to demodulate the received signal

$$\begin{aligned} Y &= Q\left(H_{cir}Q^{*}\hat{X} + n\right) = QH_{cir}Q^{*}\hat{X} + Q\boldsymbol{n} \\ &= QH_{cir}Q^{*}\hat{X} + N \end{aligned}, \qquad (2.4)$$

where N is the FFT of the AWGN vector $\boldsymbol{n}$. Then from (2.1) it can be seen that

$$\Lambda = \left(Q^{*}\right)^{-1} H_{cir}Q^{-1}. \qquad (2.5)$$

Then noticing that

$$\left(Q^{*}\right)^{-1} = Q,$$

(2.5) can then be written as

$$\Lambda = QH_{cir}Q^{*}. \qquad (2.6)$$

Substituting (2.6) into (2.4) results in,

$$Y = \Lambda\hat{X} + N.$$

Thus the received vector is the transmitted set of parallel and independent (if $\boldsymbol{n}$ is white) subchannel values with gains given by the singular values λ_n, the n^{th} diagonal element of the matrix Λ, resulting in the output for each channel Y_n

$$Y_n = \lambda_n\hat{X}_n + N_n.$$

From this it can be seen that each subchannel has its own complex gain element and thus an arbitrary and independent phase. To then recover the originally transmitted signal would require an equalizer, separate from the front end time-domain equalizer which is the focus of this thesis, for each individual subchannel, making decoder implementation extremely complex. To avoid individually equalizing every subchannel a frequency-domain equalizer (FEQ) is used. The single equalizer can adjust both the gain and phase of each subchannel making decoding easier and thus recovering the original signal. This equalizer is not the focus of this thesis; it is in addition to the TEQ equalizer.

Before closing, notice that adding the cyclic prefix does add overhead and reduces the amount of information that can be sent over the channel. In highly dispersive channels, such as that in ADSL, the length of the cyclic prefix would have to be very large, resulting in an appreciable reduction in information bit rate by a factor of $\upsilon/(N+\upsilon)$. Also if the impulse response of the channel is larger than the length of the added cyclic prefix, then energy from the previous symbol will leak into the N received symbols and the channel will no longer look circular. It is almost always the case that the channel impulse response will be longer than the pre-determined cyclic prefix length.

A solution to the above problem is to perform some front-end time-domain equalization at the receiver. The front-end equalization can effectively shorten the channel impulse response to less than υ samples, restoring the circular property

desired. This thesis addresses the critical job of creating a relatively low complexity adaptive equalizer to effectively shorten the channel impulse response.

2.3 Discrete Multitone Transmission (DMT) System

A block diagram of the basic DMT transceiver is shown in Figure 2.3. Here an input bit stream of rate R_{in} (bits/sec) is buffered into blocks of $b_{in}=R_{in}T$ bits, where T is the symbol period in seconds, resulting in b_{in} bits/symbol. Each of the b_{in} bits are then partitioned, as in Figure 2.1, to $\overline{N} \leq N/2$ subchannels by a bandwidth optimization algorithm. The bandwidth optimization algorithm is performed at startup and uses the signal-to-noise ratio (SNR) profile across the entire Nyquist bandwidth to determine $\overline{N}$, the optimum number of subchannels that should be used out of the N/2 available ones, and the optimal number of input bits, $b_{opt,i}$ allocated to each usable subchannel i. The b_{opt} bits are then assigned to each of the $\overline{N}$ subchannels and mapped to the appropriate QAM symbols to obtain the $\overline{N}$ complex subsymbols. The $\overline{N}$ complex subsymbols are then modulated by an N-point IFFT into N real symbols by imposing the Hermitian symmetry condition stated in section 2.2, and reiterated here for convenience

$$\hat{X}(0)=\Re\{X(0)\} \qquad \hat{X}\left(\frac{N}{2}\right)=\Im\{X(0)\}$$
$$\hat{X}(k)=X(k) \quad 1\le k\le\frac{N}{2}-1 \qquad . \tag{2.7}$$
$$\hat{X}(N-k)=X^{*}(k) \quad 1\le k\le\frac{N}{2}-1$$

A cyclic prefix of length υ is then added to the beginning of each input block of length N to eliminate interblock interference (IBI) in the DMT. The N+υ samples are then converted from parallel to serial, passed through a digital-to-analog converted (DAC), and transmitted over the channel.

At the receiver the channel output is sampled and passed through a time-domain equalizer (TEQ). Upon equalization, the effects of the channel are now constrained to be the length of the cyclic prefix, and the samples corresponding to the cyclic prefix can be discarded. The remaining symbol stream is then converted to parallel format, and transformed (demodulated), through an N-point FFT, to $\overline{N}$ complex subsymbols, each of which are then individually decoded.

The focus of this thesis is on the creation of the front-end time-domain equalizer, to effectively "shorten" the channel impulse response (CIR). This equalizer is to be used in DMT systems for ADSL. The ADSL system will be described next, with a focus on the specifications that will be used in the design and simulation of the channel impulse response shortening equalizer.

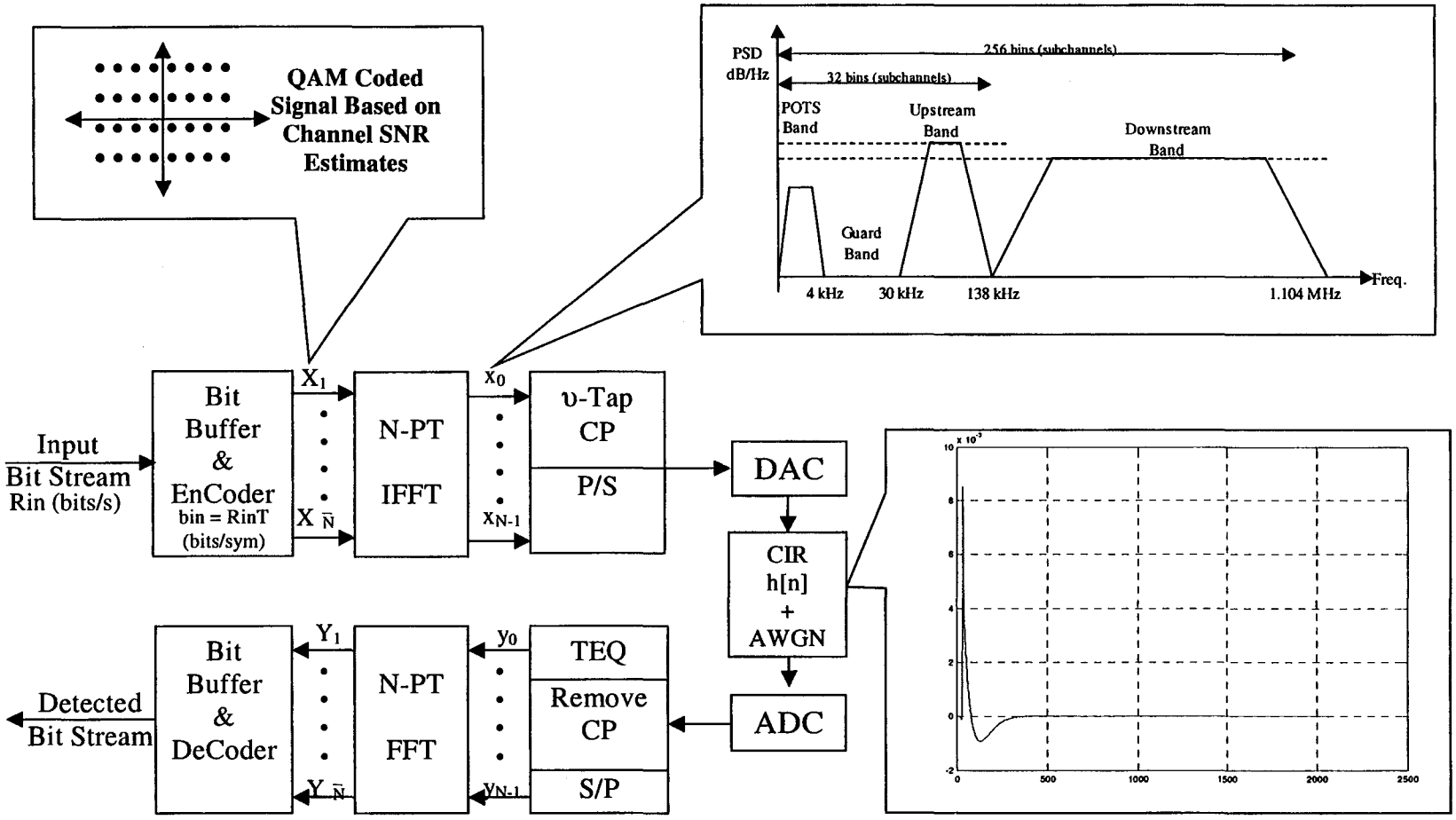

Figure 2.3 Block Diagram of the DMT Transceiver

2.4 Discrete Multitone Modulation in ADSL: Specifications

The American National Standards Institute (ANSI) T1.413 ADSL standards specify the use of the DMT as the ADSL modulation standard [5]. Asymmetric digital subscriber line (ADSL) service is a local loop transmission technology that utilizes the pre-existing copper telephone lines to provide multimedia services to the home. This technology can simultaneously support both downstream transmission, from central office to remote terminal unit (home), and upstream transmission, from remote terminal unit to central office, while unobtrusively maintaining analog voice transmission through the plain old telephone service (POTS).

The ADSL system includes an ADSL terminal unit in the central office (ATU-C), local loop, and an ADSL remote terminal unit at the customer premises (ATU-R), as shown in Figure 2.4. Downstream transmission, ATU-C to ATU-R, can transfer at bit rates up to 9Mb/s, while the upstream transmission, ATU-R to ATU-C, can deliver at bit rates up to 1 Mb/s. This downstream-to-upstream ratio of 9-to-1 is particularly well suited for TCP/IP Internet file transfers in which the bandwidth required for a request for information is much less than the bandwidth required to download large multimedia files. The term asymmetric rises from the fact that the bit rate in the downstream direction is much higher than that in the upstream for typical operations. The simulations of section 5 were run in the downstream direction only.

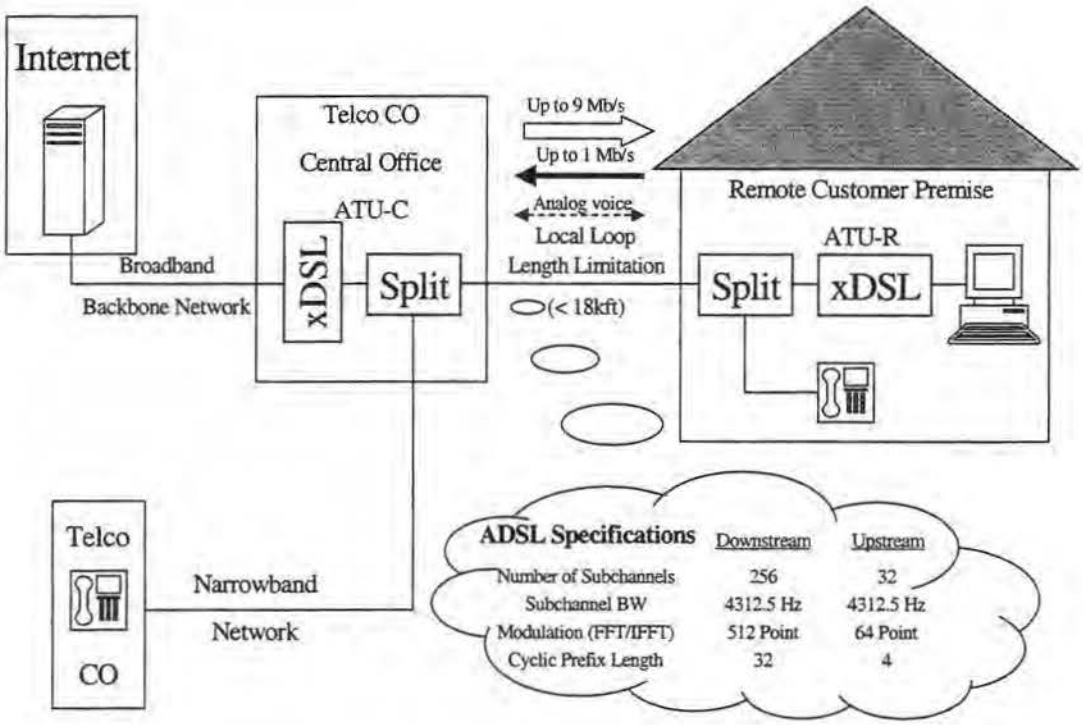

Figure 2.4 ADSL System Diagram

ADSL systems can use one of two transmission techniques, both of which are DMT based: Frequency division multiplexed (FDM) DMT or echo-canceled (ECH) DMT. The frequency division multiplexing scheme is also sometimes referred to as a frequency division duplex (FDD) DMT. The FDM transmission technique places the upstream transmission in a frequency band separate from the downstream band, as illustrated in Figure 2.5, and hence the term duplex. This method is used to help prevent self-crosstalk. The other method, ECH, allows the downstream band to overlap with the upstream band, as shown in Figure 2.6. While this technique allows the downstream channel to achieve higher data rates relative to FDM, it is subject to

the damaging self-crosstalk, which arises as a result of the echos created by simultaneous upstream and downstream transmission. As seen in Figure 2.5 and Figure 2.6, both schemes include a guard band, which is necessary to facilitate the filters that prevent the digital transmission noise from interfering with the POTS analog signal. These filters are known as the "splitters" or the "split" as seen in Figure 2.4.

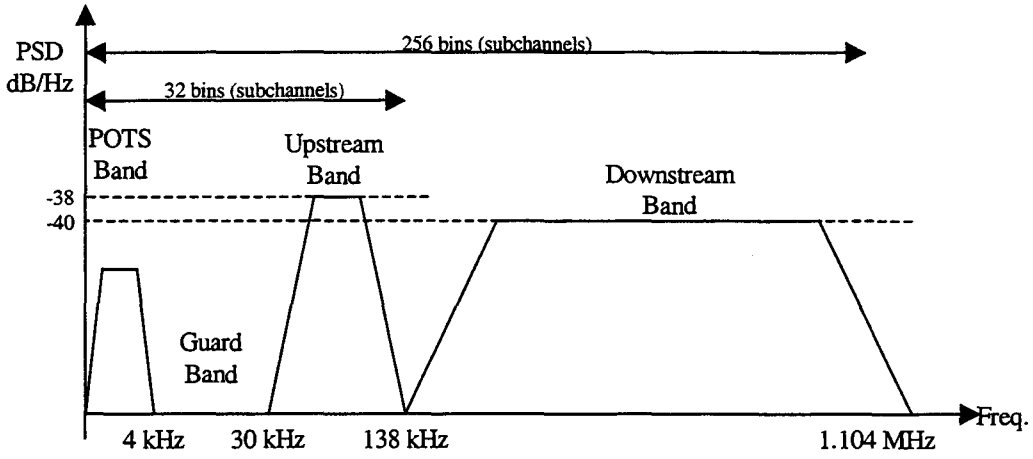

Figure 2.5 FDM ADSL

While motivated by DMT systems for ADSL, the method developed in this thesis can be used for any impulse shortening problem and thus can be used for either FDM or ECH DMT systems. The focus of this thesis is on FDM DMT systems and thus the echo-cancellation method is not addressed.

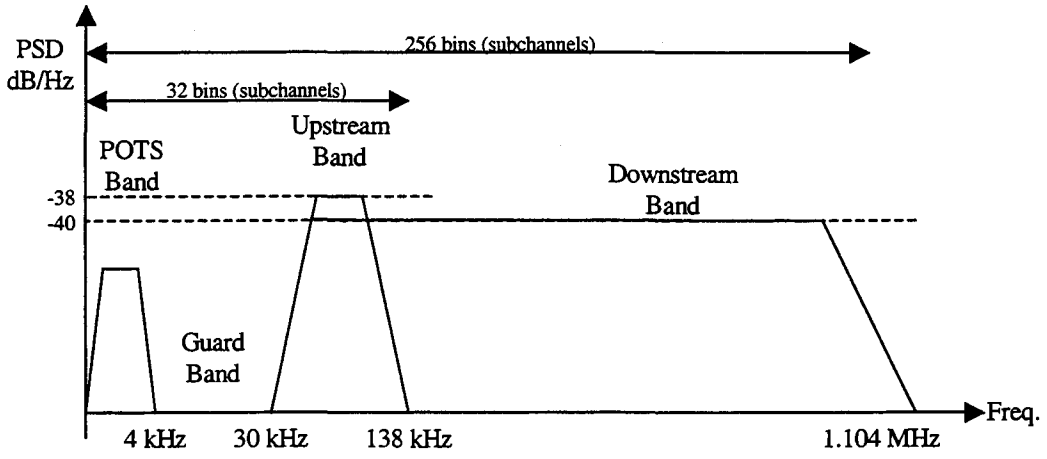

Figure 2.6 ECH ADSL

The ADSL specifications are indicated in Figure 2.5 and 2.6 and restated here. These specifications will be used in the simulations of section 5. The ADSL downstream standard specifies a sampling rate of $f_s=1/T=2.208$ MHz, with a block size of N=512, where N is as in Figure 2.3. As stated, the Hermitian symmetry condition (2.7) has to be imposed to provide a real output, thus 256 tones (subchannels) are actually transmitted from 0 to 1.104 MHz (Figure 3.2), giving a tone width (bin width) of 2.208 MHz/512=4.3125 kHz. Typically the first 7 tones contain no data to facilitate the POTS signal and appropriate guard band, as well as the last tone since this occurs at the Nyquist frequency. The cyclic prefix length is specified as being υ=32 samples. Additionally a synch symbol is inserted every 68 symbols, reducing the symbol rate to 2.208 MHz/(544×69/68)=4000 Hz. Thus the total overhead can be calculated as (4312.5-4000)/40=7.8%. The transmit power spectral

density is –40 dBm/Hz, as seen in Figure 2.5, with a tolerable variation over the tones of ±2.5 dB, giving a maximum transmit power of 20 dBm. In the simulations, the actual transmitted power will always be chosen such that the maximum power will always be less than 20 dBm to determine performance under worst case conditions.

Upstream transmission requires a sampling rate of f_s=1/T=276 kHz. The block size is set to N=64 corresponding to a total of 32 subchannels from 0 to 138 kHz. The cyclic prefix length is set to υ=4, with a synch symbol inserted every 68 symbols to give an actual symbol rate of 278 kHz/(68×68/69)=4000 Hz. The total overhead can then be written as before as (4312.5-4000)/40=7.8%. Also, the transmit power spectral density is specified at –38 dBm/Hz, Figure 2.6, with up to a 2.5 dB variation, yielding a maximum transmit power of 14 dBm. The simulations were run in only the downstream direction and thus the upstream specifications are not used but have been included for completeness.

Recall that the cyclic prefix is a critical component for effective equalization. In the downstream direction a 32-sample prefix is appended to the N=512 samples. Thus the prefix would consist of samples 480-511, giving an output of the DMT transmitter as $x_{480}, x_{481}, x_{482},\ldots\ldots, x_{511}, x_0, x_1, x_2,\ldots\ldots, x_{510}, x_{511}$. Since the actual length of the channel is much greater than the specified 32 sample prefix, partial equalization will be required to reduce the effect of the channel to the length of the cyclic prefix. This partial-equalization is accomplished through a time-domain equalizer, which is, the main focus of this thesis and is described in the following section.

3. GENERAL DMT EQUALIZATION

As indicated previously, the cyclic prefix has to be at least as long as the channel impulse response, which typically is 2048 samples for severe-ISI channels. Thus a long cyclic prefix would be required, dramatically reducing the information bit rate per frame or transmit symbol.

The goal is to use channel equalization to reduce the channel impulse response length to fit within a pre-defined cyclic prefix length. This pre-defined length has been specified in the ANSI standard as a reasonable tradeoff between the required overhead and actual achievable length to which the channel can be constrained. Such equalizers have been proposed in [1,2] to linearly equalize the channel impulse response (CIR) to a much shorter target impulse response (TIR). These equalizers limit the equalized channel response to the length of the cyclic prefix through minimization of the mean-square error (MSE).

It was found in [1] that the minimum-mean-square-error decision feedback equalizer (MMSE-DFE) could provide near optimum settings for the feed-forward and feedback filters in minimizing the mean-square error [6]. A particularly attractive feature of the decision feedback equalizer (DFE) was that it could be made adaptive, and the equalizer coefficients trained through MMSE adjustment with the LMS adaptive algorithm [7]. A drawback of the MMSE-DFE was that it required a large number of feedforward and feedback coefficients, thus increasing the overall implementation complexity. Another equalizer structure, the minimum mean-square

error input-aided equalizer (MMSE-IAE) was also suggested as an extension to the DFE [8]. The difference between this structure and the DFE is that the feedback section of the DFE does not have to being constrained to be causal and a delay can be introduced between the feedforward and feedback section to reduce the number of coefficients required. These coefficients are known as the time domain equalizer coefficients (TEQ). The MMSE-IAE equalizer is the same structure as the one proposed in this thesis, but with the delay explicitly accounted for.

The rest of the section is organized as follows: In the following section the optimum equalizer settings will be derived for the MMSE-IAE equalizer, referred to as the MMSE equalizer, subject to a unit energy constraint (UEC). It was shown in [8] that a constraint was necessary to avoid converging to the trivial solution, of which two possible constraints suggested were the unit energy constraint and a unit tap constraint (UTC). Of the two it was shown that the UEC would yield a higher output SNR [8]. The use of the POCS technique reduces this dependence of the solution on the above stated constraints. As will be seen, the solution for the MMSE-IAE equalizer requires matrix inverses to be performed and is thus not practical for real-time implementation. However it does provide what is considered the optimum solution and provides a means by which to compare the success of the proposed algorithm.

3.1 DMT Equalization Problem

The block diagram of the TEQ is shown in Figure 3.1. For a fixed TIR length, N_b, the objective is to compute the coefficients of the time-domain equalizer, $\boldsymbol{w}$, and the target impulse response, $\boldsymbol{b}$, to minimize the mean square of the error sequence

$$\min_{w,b} \mathrm{E}[e_k^2(n)],$$

where

$$e_k(n) = \boldsymbol{b}_{opt}^T \boldsymbol{x}_{k-\Delta} - \boldsymbol{w}_{opt}^T \boldsymbol{y}_k . \tag{3.1}$$

The vector $\boldsymbol{b}_{opt}$ is the length N_b vector, $\boldsymbol{b}_{opt}$= [b_0 b_1 ····· b_{Nb-1}], that represents the optimum TIR coefficients and $\boldsymbol{h}$=[h_0 h_1 ····· $h_{\upsilon-1}$] the length-υ channel impulse response where $\upsilon >> N_b$.

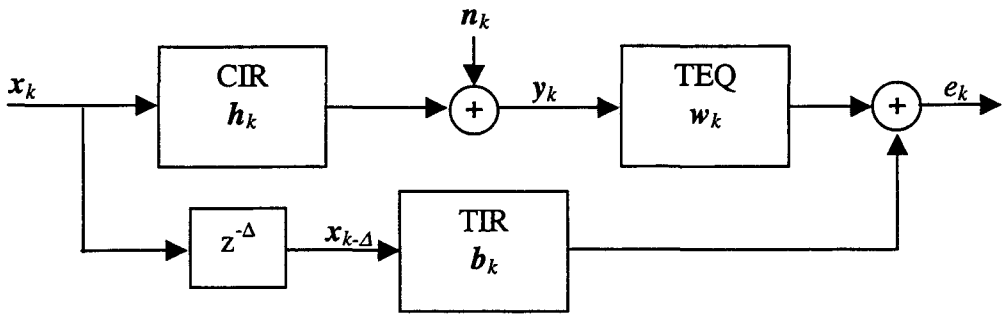

Figure 3.1 Block Diagram of the MMSE-IA Equalizer

The vector $\boldsymbol{x}_{k-\Delta}=[\ x_{k-\Delta}\ \cdots\cdots\ x_{k-\Delta-Nb}\ ]$ represents the delayed version of the received samples. For analysis, this vector of delayed channel inputs $\boldsymbol{x}_{k-\Delta}$ is assumed to be a Gaussian distributed random variable. The vector $\boldsymbol{w}_{opt} = [\ w_0\ w_1\ \cdots\cdots\ w_{Nf-1}\ ]$is the length N_f vector of optimum TEQ coefficients.

3.2 Optimum DMT Equalization

Since the channel output is simply the convolution of the CIR with the input, then the channel output sample vector $\boldsymbol{y}_k$ can be expressed in terms of the input, channel impulse response, and noise in matrix form as,

$$\begin{bmatrix} y_{k+N_f-1} \\ y_{k+N_f-2} \\ \vdots \\ y_k \end{bmatrix} = \begin{bmatrix} h_0 & h_1 & \cdots\cdots & h_v & 0 & \cdots\cdots & 0 \\ 0 & h_0 & h_1 & \cdots\cdots & h_v & 0 & \cdots \\ \vdots & & \ddots & \ddots & & \ddots & \vdots \\ 0 & \cdots & 0 & h_0 & h_1 & \cdots\cdots & h_v \end{bmatrix} \times \begin{bmatrix} x_{k+N_f-1} \\ x_{k+N_f-2} \\ \vdots \\ x_k \end{bmatrix} + \begin{bmatrix} n_{k+N_f-1} \\ n_{k+N_f-2} \\ \vdots \\ n_k \end{bmatrix}$$

or more compactly as,

$$\boldsymbol{y} = H\boldsymbol{x} + \boldsymbol{n}\,.$$

For analysis the noise vector $\boldsymbol{n}$ is assumed to be additive white Gaussian noise.

Then from the definition of the error (3.1), the mean-square error can be expressed in terms of the TIR and TEQ coefficients and statistics of the input data as

$$\begin{aligned} MSE &\overset{def}{=} E\left[\ |e_k|^2\ \right] = E\left[\ \left|\left(\boldsymbol{b}^T\boldsymbol{x}_{k-\Delta} - \boldsymbol{w}^T\boldsymbol{y}_k\right)\right|^2\ \right] \\ &= \boldsymbol{b}^T R_{xx,\Delta}\boldsymbol{b} - \boldsymbol{b}^T R_{xy,\Delta}\boldsymbol{w} - \boldsymbol{w}^T R_{xy,\Delta}\boldsymbol{b} + \boldsymbol{w}^T R_{yy}\boldsymbol{w} \end{aligned} \qquad (3.2)$$

where $R_{xy,\Delta}$ is an $(N_b+1)\times N_f$ matrix of cross-correlation coefficients

$$R_{xy,\Delta} = E[\boldsymbol{x}_{k-\Delta}\boldsymbol{y}_k{}^T] = R_{xx,\Delta}H^T,$$

and $R_{xx,\Delta}$ is an $(N_b+1)\times(N_f+\upsilon)$ matrix of autocorrelation coefficients. R_{yy} is the $N_f \times N_f$ square matrix of autocorrelation coefficients, and can be written as

$$R_{yy} = HR_{xx}H^T + R_{nn},$$

with R_{nn} also an $N_f \times N_f$ square matrix of the additive noise autocorrelation coefficients.

Then in minimizing the mean-square error in (3.2), the Orthogonality Principle is imposed [8]. This principle states that the optimal error sequence is uncorrelated with the observed data,

$$\begin{aligned} E[\boldsymbol{e}_k \boldsymbol{y}_k^T] &= 0 \\ E[(\boldsymbol{b}_k^T \boldsymbol{x}_{k-\Delta} - \boldsymbol{w}_k^T \boldsymbol{y}_k)\boldsymbol{y}_k^T] &= 0 \\ E[\boldsymbol{b}_k^T \boldsymbol{x}_{k-\Delta}\boldsymbol{y}_k^T - \boldsymbol{w}_k^T \boldsymbol{y}_k \boldsymbol{y}_k^T] &= 0 \end{aligned}$$

giving,

$$\boldsymbol{b}_k^T R_{xy} = \boldsymbol{w}_k^T R_{yy} \tag{3.3}$$

Then solving for $\boldsymbol{w}_k$ in (3.3) and substituting into (3.2), with some simplification, results in the following expression for the MSE,

$$MSE = \boldsymbol{b}_k^T R_{TEQ,\Delta} \boldsymbol{b}_k$$

where

$$R_{TEQ,\Delta} = \tilde{R}_{xx,\Delta} - R_{xy,\Delta}R_{yy}{}^{-1}R_{xy,\Delta}.$$

Note that $\tilde{R}_{xx,\Delta} = E[\boldsymbol{x}_{k-\Delta}{}^T \boldsymbol{x}_{k-\Delta}] \neq R_{xx,\Delta}$ is an $(N_b+1)\times(N_b+1)$ square matrix. The value of $\boldsymbol{b}$ that minimizes the MSE, $\boldsymbol{b}_{opt}$, is the eigenvector corresponding to the smallest eigenvalue of the matrix $R_{TEQ,\Delta}$, subject to a UEC [8].

$$\boldsymbol{b}_{opt} = \arg\min_{\boldsymbol{b}} \boldsymbol{b}^T R_{TEQ,\Delta} \boldsymbol{b}\,.$$

The UEC has to be imposed to avoid $\boldsymbol{b}_{opt}$ converging to the trivial solution ($\boldsymbol{b}_{opt}=\mathbf{0}$), and thus $\boldsymbol{w}_{opt}$ also converging to the trivial solution. Finally, from (3.3), the minimum mean-square error (MMSE) finite-length TEQ can be computed from

$$\boldsymbol{w}_{opt} = \boldsymbol{b}_{opt} R_{xy,\Delta} R_{yy}^{-1}\,.$$

Note that the optimum TIR, $\boldsymbol{b}_{opt}$, may need to be solved for all the values of Δ, $0 \le \Delta \le N_f + \upsilon - N_b - 1$, to find the MMSE. This need for an exhaustive search procedure to find the optimum delay and the need to perform the matrix inverse, a computationally intensive procedure, has prompted the need for time-recursive techniques, the focus of the following section, the results of which will be compared against the optimum solution found in this section. Again, notice that the use of the POCS and RLS algorithm will not require the exhaustive search procedure or the UEC to reach a solution.

4. RECURSIVE LEAST SQUARES-PROJECTION ONTO CONVEX SETS (RLS-POCS) EQUALIZATION SOLUTION

As mentioned, the goal of the MMSE equalizer is to limit the equalized channel response to be of the same, fixed length as the cyclic prefix. In so doing we are reducing the required transmission overhead, and thus increasing the rate of information transmission. The MMSE equalization problem involves a dual optimization problem, specifically the optimization of both the TIR and the TEQ. As seen in section 3.2, finding the optimum solutions directly involves solving for matrix inverses, which is computationally intensive and not appropriate for on-line implementation. Although non-iterative solutions for solving the matrix inverse have been proposed [3,4,6,9], this section will deal with finding a time-recursive solution for the matrix inverse that is adaptive and naturally extends to channels of a more time-varying nature.

The solution proposed in [1] uses an adaptive gradient-based least-mean-square (LMS) algorithm. LMS is a statistically based adaptive algorithm that is based on gradient descent. It is known to suffer from slow convergence, as well as a high level of residual error upon convergence as verified by the results in [4]. The rate of convergence of the output MSE of the LMS gradient adaptive equalizer is directly related to the eigenvalue spread of the input covariance matrix. If the spread is large, the convergence will be very slow. This slow convergence is due to the single step size parameter in the LMS gradient algorithm. While a number of methods have been proposed for independently updating the step size, a faster convergence rate can be

achieved when the error measure is expressed in terms of a time average of the actual received signal instead of a statistical or ensemble average. These data error-based algorithms are collectively known as the recursive least squares (RLS) algorithms. The solution the RLS algorithm provides is based on Newton-type methods and thus does not suffer from the slow convergence or large residual MSE inherent in the LMS (steepest descent-based) algorithm.

As mentioned the DMT equalizer solution is a joint optimization problem, meaning that the optimum TEQ depends on the chosen TIR and vice versa. The difficulty arises from the fact that in order to use the RLS algorithm, the TIR used to calculate the TEQ has to be of the same length. Thus a method had to be found which could jointly calculate the optimum TEQ, calculated from an equal length TIR, and then constrain the TIR to the pre-determined length. Also since one of the goals is to reduce the required convergence time, through use of the RLS, it would be advantageous to find a technique that could satisfy these constraints in a minimal amount of time. The POCS technique was chosen due to the projection-like matrices found in solving for the optimum solution and how the shortened TIR formed a convex set over the range of interest. The idea of forming a convex set is an import property in guaranteeing that the method will provide a convergent solution, and thus the reason the POCS method was chosen to satisfy the constraint length requirement. Also, as will be seen, the POCS method was able to satisfy these constraints in a single iteration, and thus not reducing the gains achieved through use of the RLS algorithm.

4.1 General Recursive Least Squares Adaptive Equalization

The general RLS problem requires finding the tap gain vector of the equalizer $w(n)$ ($w(n) \neq$ TEQ coefficients) such that the cumulative least squared error measure, $J(n)$, is minimized [11],

$$J(n)=\sum_{i=1}^{n}\lambda^{n-i}\left|e^{2}(i,n)\right|$$

the weighting factor, λ also known as the fade factor, weights the most recent data more heavily and typically lies in the interval $.95<\lambda<.9995$, depending on the statistics of the input, $x(i)$. For a typical system identification configuration, as shown in Figure 4.1, the error $e(i,n)$, at each time i given the filter weights at current time n, is defined as

$$e(i,n)=d(n)-\mathbf{x}_N^T(n)\mathbf{w}_N(n) \qquad 1\leq i\leq n$$

where $d(n)$ is the desired output, $w(n)$ is the new tap gain vector at time n, and $\mathbf{x}_N^T(n)\mathbf{w}_N(n)$ is the estimate of the desired signal, $\hat{d}(n)$.

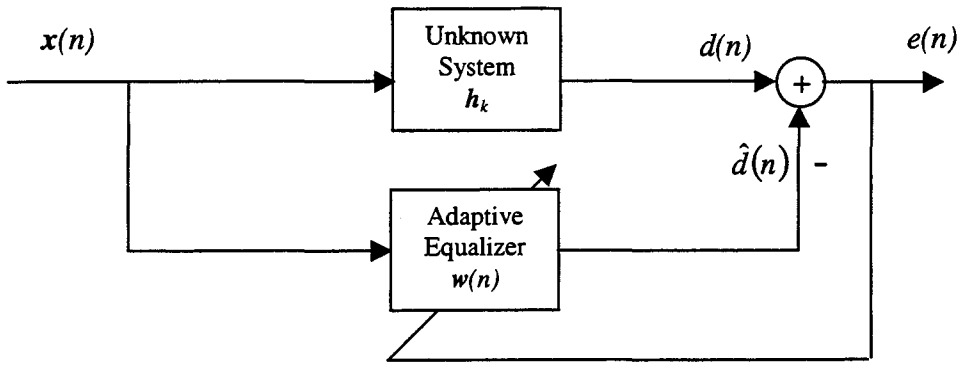

Figure 4.1 RLS Weight Update Block Diagram

4.2 Recursive Least Squares-Projection onto Convex Sets (RLS-POCS)

The remainder of this section will deal with the application of the previously outlined general RLS error minimization procedure, to the DMT equalizer as shown in Figure 4.2.

As will be seen the algorithm will progress in 3 steps. First, in section 4.2.1, the optimum TEQ will be solved for using the RLS weight update procedure in terms of the TIR. In section 4.2.2, the optimum TIR will be found in terms of the previously found TEQ, and the TIR constrained to the fixed cyclic prefix length in section 4.2.3 using the POCS method. Finally at the end of section 4.2.3, the dual constrained RLS-POCS optimization algorithm will be outlined.

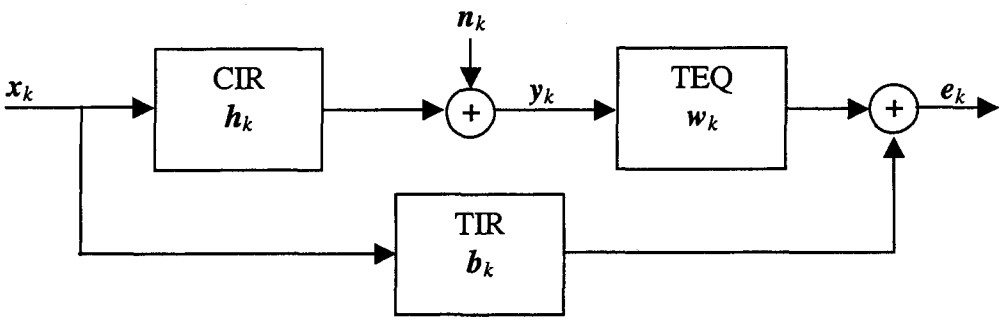

Figure 4.2 Block Diagram of DMT Equalizer

4.2.1 Optimum TEQ

It is a simple extension to apply the general RLS error minimization problem in Figure 4.1 to the DMT equalizer (Figure 4.2), as shown in Figure 4.3.

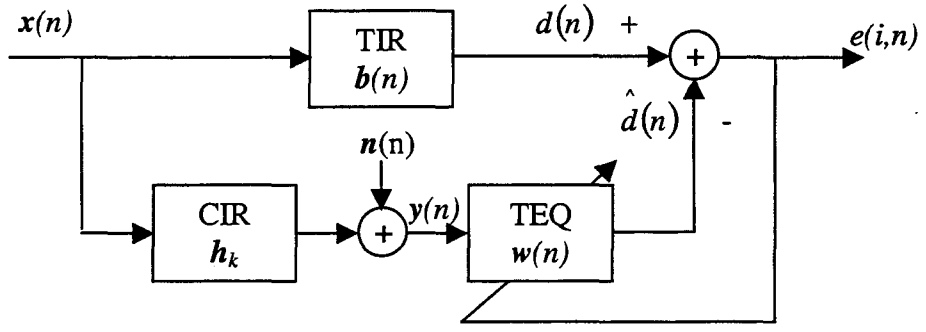

Figure 4.3 RLS DMT Equalizer Block Diagram

Defining the output error

$$\begin{aligned} e(i,n) &= d(i) - \hat{d}(i) \\ &= \boldsymbol{x}^T(i)\boldsymbol{b}(n) - \boldsymbol{y}^T(i)\boldsymbol{w}(n) \end{aligned} \tag{4.1}$$

where $\boldsymbol{y}^T(i) = [\, y(i)\ y(i-1)\ \cdots\ y(n-N_f+1)\,] = H\boldsymbol{x}^T(n) + \boldsymbol{n}(n)$ is the $N_f \times 1$ channel output vector at time i, $\boldsymbol{x}^T(i) = [x(i)\ x(i-1)\ \cdots\ x(n-N_f+1)\,]$ is the $N_f \times 1$ input vector at time i, and $\boldsymbol{w}(n)$, $\boldsymbol{b}(n)$ comprise the adaptive $N_f \times 1$ TEQ and TIR coefficient vectors respectively at time n. Here $\boldsymbol{b}(n)$ is assumed to be given and the length of the TIR coefficient vector will be constrained later using POCS in section 4.2.3 to be the required cyclic prefix length. The cumulative squared-error measure can then be written

$$\begin{aligned} J(n) &= \sum_{i=1}^{n} \lambda^{n-i} \left| e^2(i,n) \right| \\ &= \sum_{i=1}^{n} \lambda^{n-i} \left(d(i) - \boldsymbol{y}^T(i)\boldsymbol{w}(n) \right)^2 \\ &= \sum_{i=1}^{n} \lambda^{n-i} d^2(i) - 2\sum_{i=1}^{n} \lambda^{n-i} d(i)\boldsymbol{y}^T(i)\boldsymbol{w}(n) + \sum_{i=1}^{n} \lambda^{n-i} \boldsymbol{w}^T(n)\boldsymbol{y}(i)\boldsymbol{y}^T(i)\boldsymbol{w}(n) \end{aligned} \tag{4.2}$$

To obtain the minimum of the least-square error with respect to the adaptive TEQ weights, the partial-derivative of J(n) is set to zero (or equivalently apply orthogonality condition),

$$\frac{\partial}{\partial w} J(n) = 0.$$

Then using (4.1-4.2) it can be shown that

$$R_{yy}(n)\boldsymbol{w}(n) = \boldsymbol{p}(n),$$

where $\boldsymbol{w}(n)$ is the TEQ tap gain vector of the RLS equalizer at iteration n.

The matrix $R_{yy}(n)$ is an $N_f \times N_f$ matrix of input correlation coefficients to the TEQ,

$$R_{yy}(n)=\sum_{i=1}^{n}\lambda^{n-i}y(i)y^{T}(i) \tag{4.3}$$

and $\boldsymbol{p}(n)$ is the crosscorrelation vector between the inputs of the equalizer $\boldsymbol{y}(n)$ and the desired output $d(i)$, where $d(i)=\boldsymbol{x}^{T}(i)\boldsymbol{b}(n)$,

$$\boldsymbol{p}(n)=\sum_{i=1}^{n}\lambda^{n-i}d(i)\boldsymbol{y}^{T}(i). \tag{4.4}$$

Note the dependance of $d(i)$ on $\boldsymbol{b}$, thus explicitly showing the joint relationship between the optimum TEQ and TIR coefficients. Finally to compute the optimum TEQ equalizer weight vector requires calculating the matrix inverse

$$\boldsymbol{w}_{opt}(n)=R_{yy}^{-1}(n)\boldsymbol{p}(n).$$

From the definition of the input correlation coefficient matrix $R_{yy}(n)$, it is possible to write (4.3) as a recursive function

$$R_{yy}(n)=\lambda R_{yy}(n-1)+y(n)y^{T}(n). \tag{4.5}$$

Since the terms in (4.5) are all $N_f \times N_f$ dimensional, the matrix inverse lemma [12] can be invoked to derive a recursive update for the input correlation matrix $R_{yy}^{-1}(n)$ in terms of the previous inverse $R_{yy}^{-1}(n-1)$,

$$R_{yy}^{-1}(n)=\frac{1}{\lambda}\left[R_{yy}^{-1}(n-1)-\frac{R_{yy}^{-1}(n-1)y(n)y^{T}(n)R_{yy}^{-1}(n-1)}{\lambda+\mu(\mathrm{n})}\right], \tag{4.6}$$

where

$$\mu(\mathrm{n})=y^{T}(n)R_{yy}^{-1}(n-1)y(n).$$

Then based on (4.6), the RLS minimization leads to the following TEQ equalizer weight update equation

$$w_{opt}(n) = w(n-1) + g(n)e(n),$$

where

$$g(n) = \frac{R_{yy}^{-1}(n-1)y(n)}{\lambda + \mu(n)},$$

the $N_f \times 1$ dimensional input gain vector.

The steps in the RLS-TEQ equalizer update algorithm can then be summarized as follows:

RLS-TEQ Equalizer Coefficient Update

1. Initialize $y(0)=0$, $R_{yy}^{-1}(0) = \delta I_{N_f \times N_f}$, where $I_{N_f \times N_f}$ is the $N_f \times N_f$ identity matrix with $\delta >> 1$, $b(0)=w(0)=sqrt(N_f)*ones(1,N_f)$. (4.7)

2. Calculate the error based on previously calculated TIR, $b(n-1)$:

$$\begin{aligned} e(n) &= d(n) - y^T(n)w(n-1) \\ &= x^T(n)b(n-1) - y^T(n)w(n-1) \end{aligned} \quad (4.8)$$

3. Calculate the scale factor:

$$\mu(n) = y^T(n)R_{yy}^{-1}(n-1)y(n) \quad (4.9)$$

4. Calculate the gain:

$$g(n) = \frac{R_{yy}^{-1}(n-1)y(n)}{\lambda + \mu(n)} \quad (4.10)$$

5. Determine the optimum TEQ equalizer updated weights:

$$w_{opt}(n) = w_{opt}(n-1) + g(n)e(n) \quad (4.11)$$

6. Update the correlation matrix:

$$R_{yy}^{-1}(n) = \frac{1}{\lambda}\left[R_{yy}^{-1}(n-1) - g(n)y^T(n)R_{yy}^{-1}(n-1)\right] \quad (4.12)$$

7. Compute the optimum TIR ($\boldsymbol{b}_{opt}(n)$) as determined in the next section (section 4.2.2).
8. Project $\boldsymbol{b}_{opt}(n)$ onto constrained length vector $\hat{\boldsymbol{b}}(n)$as determined in section 4.2.3.
9. Return to step (2) and repeat.

Note the initialization of the TEQ and TIR coefficient vector. Initialization is necessary to avoid converging to the trivial solution as will be seen later in section 4.2.3. Also note the dependence on the prior TIR, which will be covered in the next section.

4.2.2 Optimum TIR

As seen in the previous section the DMT equalization problem is a dual constrained optimization procedure in which the optimum solution for the TEQ is directly related to the optimum solution of the TIR, with the TIR being subject to a pre-determined constraint length. Thus, following each iteration of the RLS update, summarized in (4.7-4.12), the optimum TIR, $\boldsymbol{b}_{opt}(n)$, must also be computed in terms of $\boldsymbol{w}_{opt}(n)$ found in (4.11). Thus, writing the mean squared-error measure from the error defined in (4.8)

$$
\begin{aligned}
MSE &= E[|e^2(n)|] \\
&= E\left[\left|\left(x^T(n)b(n) - y^T(n)w_{opt}(n)\right)^2\right|\right] \\
&= b^T(n)R_{xx}(n)b(n) - 2b^T(n)x^T(n)y(n)w_{opt}^T(n) + w_{opt}^T(n)R_{yy}(n)w_{opt}(n)
\end{aligned}
$$

Setting the partial-derivative, with respect to the TIR weights, to zero

$$\frac{\partial}{\partial b} MSE = 0$$

results in

$$b(n)R_{xx}(n) = \hat{p}(n)$$

$$b_{opt}(n) = R_{xx}^{-1}(n)\hat{p}(n)$$

where $b_{opt}(n)$ is the optimal TIR weight vector at iteration n of size $N_f \times 1$, the $N_f \times N_f$ input correlation matrix

$$R_{xx}(n) = x(n)x^T(n), \tag{4.13}$$

and the $N_f \times 1$ TEQ input correlation vector

$$\hat{p}(n) = \hat{d}(i)x(n),$$

where $\hat{d}(i) = y^T(i)w(n)$, again explicitly showing the relationship between the optimum TEQ and TIR weight vector. Then (4.13) can be written as a recursive equation

$$R_{xx}^{-1}(n) = R_{xx}^{-1}(n-1) + x(n)x^T(n). \tag{4.14}$$

Since all elements of (4.14) involve an $N_f \times N_f$ matrix, the matrix inverse lemma can again be used to avoid directly performing the matrix inverse of (4,13), thus giving

$$R_{xx}^{-1}(n) = R_{xx}^{-1}(n-1) - \frac{R_{xx}^{-1}(n-1)x(n)x^T(n)R_{xx}^{-1}(n-1)}{1 + x^T(n)R_{xx}^{-1}(n-1)x(n)}. \tag{4.15}$$

As before, the gain factor can be written as

$$gg(n)=\frac{R_{xx}^{-1}(n-1)x(n)}{1+\kappa(n)}$$

where

$$\kappa(n)=x^T(n)R_{xx}^{-1}(n-1)x(n),$$

substituting into (4.15)

$$\begin{aligned}R_{xx}^{-1}(n)&=R_{xx}^{-1}(n-1)-gg(n)x^T(n)R_{xx}^{-1}(n-1)\\&=R_{xx}^{-1}(n-1)\left[1-gg(n)x^T(n)\right]\end{aligned}$$

From these recursive equations, the optimum TIR, based on the previously found TEQ, can be written

$$b_{opt}(n)=b(n-1)-gg(n)x^T(n)b(n-1)+\hat{d}(n)gg(n).$$

Noticing that

$$\hat{e}(n)=y^T(n)w_{opt}(n)-x^T(n)b(n-1),$$

the final optimum TIR equation can be written

$$b_{opt}(n)=b(n-1)-gg(n)\hat{e}(n). \tag{4.16}$$

Thus, the steps in solving for the optimum TEQ and TIR are summarized below:

RLS-TEQ and TIR Equalizer Coefficient Update

1. Initialize x(0)=0, $R_{xx}^{-1}(0)=\delta I_{N_f\times N_f}$, where $I_{N_f\times N_f}$ is the N_f×N_f identity matrix with δ>>1.
2. Complete (4.7-4.12) to compute the optimum TEQ ($w_{opt}(n)$) at iteration n. (4.17)

3. Calculate the scale factor:

$$\kappa(n) = \kappa^{T}(n) R_{xx}^{-1}(n-1) x(n) \tag{4.18}$$

3. Calculate the gain factor:

$$gg(n) = \frac{R_{xx}^{-1}(n-1) x(n)}{1 + \kappa(n)} \tag{4.19}$$

4. Calculate the error based on previously calculated $w_{opt}(n)$:

$$\hat{e}(n) = y^{T}(n) w_{opt}(n) - x^{T}(n) b(n-1) \tag{4.20}$$

5. Determine the equalizer updated weights:

$$b_{opt}(n) = b(n-1) + gg(n) \hat{e}(n) \tag{4.21}$$

6. Update the input correlation matrix:

$$R_{xx}^{-1}(n) = R_{xx}^{-1}(n-1) - gg(n) x^{T}(n) R_{xx}^{-1}(n-1) \tag{4.22}$$

7. Project $b_{opt}(n)$ (4.21) onto constrained length vector $\hat{b}(n)$ as determined in next section (section 4.2.3).

8. Return to step 2 and repeat.

4.2.3 Projection onto Convex Sets

Up to this point the constraint length of the TIR has not been addressed. As stated in section 2.2 the cyclic prefix plays a vital role in the operation of the DMT. In

order to reduce the required overhead due to the cyclic prefix, the TEQ is incorporated into the DMT receiver design to force a long channel impulse response into an equivalent short length TIR. The length of the TIR is referred to as the constraint length.

Notice that at the end of every iteration, equation (4.21) is the same length as the TEQ. In order to constrain the length of the TIR, the method of projections onto convex sets (POCS) is employed. This vector-space projection technique always provides a solution consistent with a given set of constraints.

A set C is considered convex if

$$x = \mu x_1 + (1-\mu)x_2 \in C \qquad \text{for all } x_1, x_2 \in C,\ 0 \le \mu \le 1. \qquad (4.23)$$

In words, if a set has the property that all points on a line segment joining any two points in the set is also in the set, then that set is said to be convex.

For the optimum equalization of DMT problem the constraint set C_1, consists of all the points in the N_b (N_b =TIR Constraint Length) dimensional Euclidean space

$$C_1 : \left\{ \hat{\boldsymbol{b}} \in R^{N_f} : \left[\boldsymbol{b}^T_{N_b \times 1} \quad \boldsymbol{0}_{1 \times (N_f - N_b)} \right] \right\}$$

where $\boldsymbol{0}_{\times}$ is the $\times$-dimensional vector comprising all zeros.

For the method of projection onto constraint sets to be valid, it must be shown that the constraint set C_1 is a closed and convex set. In other words, if $\boldsymbol{b}$ (defined below using (4.23)) is an element of the line defined by the points $\boldsymbol{b}_1$ and $\boldsymbol{b}_2$ then C_1 is convex,

$$\boldsymbol{b} = \mu \boldsymbol{b}_1 + (1-\mu)\boldsymbol{b}_2 \in C_1 \qquad \text{for all } \boldsymbol{b}_1, \boldsymbol{b}_2 \in C_1,\ 0 \le \mu \le 1.$$

Note that since $\boldsymbol{b}_1$ and $\boldsymbol{b}_2$ have the last $(N_f - N_b)$ elements as zeros, then $\boldsymbol{b} = \mu \boldsymbol{b}_1 + (1-\mu)\boldsymbol{b}_2$ also will always have the last $(N_f - N_b)$ elements be zero, and the set C_1 is indeed a convex set. Also since the Euclidean space R^{Nf} is complete [13] with respect to the norm induced by the inner product, this constraint set will form a closed set on the Hilbert space H [14].

Then for each $\boldsymbol{b}$ in H, there will be a point $\boldsymbol{a}$ in the set such that

$$\left\| \boldsymbol{b}_{opt} - \hat{\boldsymbol{b}} \right\| = \min_{\boldsymbol{a} \in C_1} \left\| \boldsymbol{b}_{opt} - \boldsymbol{a} \right\|,$$

where $\boldsymbol{b}_{opt}$ represents the optimum solution found in (4.21) and $\hat{\boldsymbol{b}}$ is the $N_b \times 1$ constrained length vector. Thus, given a point $\boldsymbol{b}_{opt}$ in the R^{Nf} dimensional Euclidean space, the projection of this point onto the constraint set C_1 would be a point $\hat{\boldsymbol{b}}$ in the set such that it minimizes the distance $\left\| \boldsymbol{b}_{opt} - \hat{\boldsymbol{b}} \right\|$, the inner product norm, written as

$$\hat{\boldsymbol{b}} = \arg \min_{\boldsymbol{a} \in C_1} \left\| \boldsymbol{b}_{opt} - \boldsymbol{a} \right\|. \tag{4.24}$$

The value of $\boldsymbol{a}$ which will satisfy (4.24) is the vector $\boldsymbol{a}$ such that

$$\left\langle \left(\boldsymbol{b}_{opt} - \boldsymbol{a} \right), \boldsymbol{a} \right\rangle = 0, \tag{4.25}$$

the value that is perpendicular to the difference vector $\boldsymbol{b}_{opt}$-$\boldsymbol{a}$. Then expanding the inner product (4.25) results in

$$\left(\boldsymbol{b}_{opt_0} - \boldsymbol{a}_0 \right) \boldsymbol{a}_0 + \left(\boldsymbol{b}_{opt_1} - \boldsymbol{a}_1 \right) \boldsymbol{a}_1 + \cdots \cdots + \left(\boldsymbol{b}_{opt_{N_f}} - \boldsymbol{a}_{N_f} \right) \boldsymbol{a}_{N_f} = 0.$$

But the vector $\boldsymbol{a}$ is constrained to be in the R^{Nb} dimensional Euclidean space, thus $a_i = 0,\ i > N_b$ giving

$$(b_{opt\,0} - a_0)a_0 + (b_{opt_1} - a_1)a_1 + \cdots \cdots + (b_{opt\,N_b} - a_{N_b})a_{N_b} = 0.$$

From which two solutions may exist:

1. $a_i = 0 \quad i \le N_b$ (Trivial Solution)
2. $a_i = b_i \quad i \le N_b$

The POCS method will only converge to the trivial solution if and only if $\boldsymbol{b}_{opt} = \boldsymbol{0}_{1\times N_f}$, and thus only if $\boldsymbol{w}_{opt} = \boldsymbol{0}_{1\times N_f}$, which will happen if either the TIR or TEQ is initialized to 0. But the constraint set C_1 does not include the origin, because any projection onto C_1 (from outside of C_1) would be on the boundary of the constraint set, and thus the origin can not be among the local minima. The projection operator can then be defined as follows

$$\hat{\boldsymbol{b}} = \begin{cases} \boldsymbol{b}_{opt} & \text{if } \boldsymbol{b}_{opt} \in C_1 \\ \boldsymbol{b}_{opt_{Nb\times 1}} & \text{if } \boldsymbol{b}_{opt} \notin C_1 \end{cases}. \tag{4.26}$$

In other words, given a vector $\boldsymbol{b}_{opt} \notin C_1$ the projection onto the constraint set would simply be the first N_b values of the optimum TIR coefficient vector found in (4.26), with the rest of the elements set equal to zero

$$\hat{\boldsymbol{b}} = [\, b_{opt_1} \cdots b_{opt_{N_b}}\ \boldsymbol{0}_{(N_f - N_b)}\,].$$

It is important to notice that while the final solution may seem trivial, this is only provided by the TIR satisfying the convex set requirements. By the TIR being a

convex set we can assure a unique solution and thus the overall convergence of the solution.

Thus, to summarize the steps in determining the constrained length TIR and optimum TEQ equalizer coefficients:

RLS-POCS Equalizer Coefficient Update Algorithm

1. Initialize x(0)=0, $b(0)=w(0)=sqrt(N_f)*ones(1,N_f)$, $R_{xx}^{-1}(0)=\delta I_{N_f\times N_f}$, $R_{yy}^{-1}(0)=\delta I_{N_f\times N_f}$, where $I_{N_f\times N_f}$ is the N_fxN_f identity matrix with δ>>1.
2. Calculate the optimum TEQ coefficients w_{opt} as outlined in (4.8-4.12)
   a.) $e(n)=x^T(n)b(n-1)-y^T(n)w(n-1)$
   b.) $\mu(n)=y^T(n)R_{yy}^{-1}(n-1)y(n)$
   c.) $g(n)=\frac{R_{yy}^{-1}(n-1)y(n)}{\lambda+\mu(n)}$
   d.) $w_{opt}(n)=w_{opt}(n-1)+g(n)e(n)$
   e.) $R_{yy}^{-1}(n)=\frac{1}{\lambda}\left[R_{yy}^{-1}(n-1)-g(n)y^T(n)R_{yy}^{-1}(n-1)\right]$
3. Calculate the TIR coefficients b_{opt} as outlined in (4.18-4.22) using w_{opt} found in step 2.
   a.) $\kappa(n)=\kappa^T(n)R_{xx}^{-1}(n-1)x(n)$
   b.) $gg(n)=\frac{R_{xx}^{-1}(n-1)x(n)}{1+\kappa(n)}$
   c.) $\hat{e}(n)=y^T(n)w_{opt}(n)-x^T(n)b(n-1)$

d.) $\boldsymbol{b}_{opt}(n) = \boldsymbol{b}(n-1) + \boldsymbol{g}\boldsymbol{g}(n)\hat{e}(n)$

e.) $R_{xx}^{-1}(n) = R_{xx}^{-1}(n-1) - \boldsymbol{g}\boldsymbol{g}(n)\boldsymbol{x}^T(n)R_{xx}^{-1}(n-1)$

4. Project the TIR coefficients (4.26) found in step 2 to find the constrained length coefficients $\hat{\boldsymbol{b}}$.

a.) $$\hat{\boldsymbol{b}} = \begin{cases} \boldsymbol{b}_{opt} & \text{if } \boldsymbol{b}_{opt} \in C_1 \\ \boldsymbol{b}_{opt_{Nbx1}} & \text{if } \boldsymbol{b}_{opt} \notin C_1 \end{cases}$$

5. Return to step 2 and repeat until end of training session.

4.3 Summary

In this section an algorithm was derived to perform the front-end time-domain equalization necessary to reduce the effects of the channel to that of a much shorter constrained length channel. The challenge of the channel impulse response-shortening problem is the dual optimization of both the TEQ and TIR equalizer coefficients with the TIR subject to a constraint length.

The RLS algorithm was utilized to provide a solution, for the TEQ, that was not subject to the long convergence times and high residual MSE found with the LMS algorithm. Then the matrix inverse lemma was used to determine the optimal N_f - length TIR coefficients, given the newly computed TEQ coefficients found using the RLS algorithm. The POCS projection technique was then used which could satisfy the need to jointly optimize the TEQ and TIR, while subject to a constraint length, thus allowing the calculation of the TEQ to be the optimum solution. As seen the

POCS method provided a simple and unique solution to a complex problem, and did so in a very computationally efficient manner. The next section contains the simulations to verify the performance of the proposed algorithm in an ADSL DMT system.

5. RESULTS

The simulation results of the RLS-POCS algorithm derived in section 4 will be presented in this section as applied to an ADSL system. As such, section 5.1 will cover the basics of the ADSL system necessary for simulation, which will include descriptions and modeling of all channel and noise impairments. Section 5.2 will then contain the simulation results based on the RLS-POCS algorithm. Finally in section 5.3 a complexity analysis will be performed to evaluate the success of the proposed algorithm, including a comparison against the computational requirements of the LMS algorithm.

5.1 ADSL Transmission Characteristics

As mentioned, ADSL is a high-speed data transmission service. The ADSL service achieves its highest transmission rates on lines within the carrier serving area (CSA), and provides a lower speed service to lines outside of the CSA called the Revised Resistance Design (RRD) loops. Typical impairments in the CSA and RRD data transmission channels include the following:

1. Intersymbol interference (ISI) from the channel.
2. Crosstalk noise coupled from adjacent loops within the same cable bundle.
3. Electronics noise, which includes thermal and quantization noise.

4. Echo noise.

5. AM radio frequency noise.

Specifically the ISI and associated channel modeling for CSA and RRD loops are covered in section 5.1.1, while section 5.1.2 will cover the crosstalk and electronics noise models. The echo noise is not in general included in FDM equalizer design simulations, as it is not a problem, and thus is not included here. For more information on echo noise and its effects on the ADSL system see [15]. Finally, the AM radio frequency noise, like the echo noise, also is not included in the simulations.

Typically the equalizer compensates for ISI, but not for the electronics and crosstalk noise. Thus the ISI is modeled in the channel impulse response $\boldsymbol{h}$, whereas the electronics and crosstalk noise are used in creating $\boldsymbol{n}$.

5.1.1 ADSL Channel Modeling

The set of loops defined for testing in an ADSL environment are given in Figures 5.1 and 5.2. These loops have been specified by both ANSI and ETSI standards committees [16], and are representative of some of the worst, in terms of channel impulse response, loops expected to be found. In general, smaller wire size, longer wire length, and more and longer bridge taps result in the overall degradation of the line and will subsequently lead to poor achievable data rates.

The first set of loops includes those without load coils, which conform to the Revised Resistance Design (RRD) rules specified by ANSI, as shown in Figure 5.1. It

can be seen that these include both 24- and 26-gauge wires in excess of 12,000 feet with multiple bridge taps.

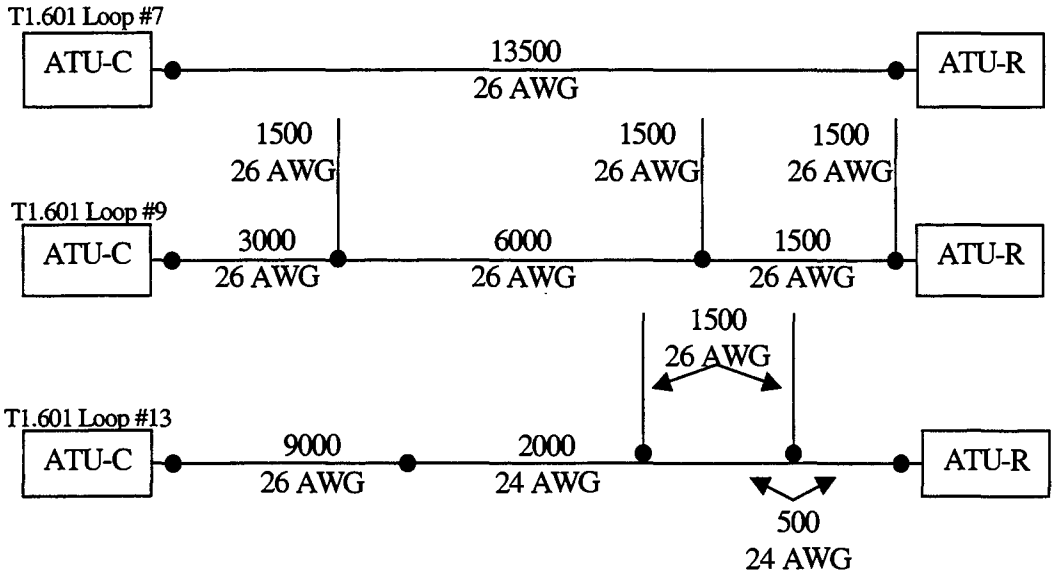

Figure 5.1 ADSL RRD Test Loops (Note: Lengths are in Feet, AWG=American Wire Gauge)

The second set of loops, include those loops within the carrier serving area (CSA) requirements also specified by ANSI, as shown in Figure 5.2. CSA loops are shorter than RRD loops with a maximum length of 12,000 feet, and also include 24- and 26-gauge wire. Also included is a mid-CSA loop that was contrived by ANSI, but does not conform to service provider deployment rules.

The channel impulse responses used in the simulations were created using a line simulation program, based on standard transmission line modeling of the

aforementioned loops. Unless specified, the simulations will be performed using CSA loop 6, for which the unit impulse and magnitude response are shown in Figure 5.3, and which represents the worst of the loops found within the CSA loops.

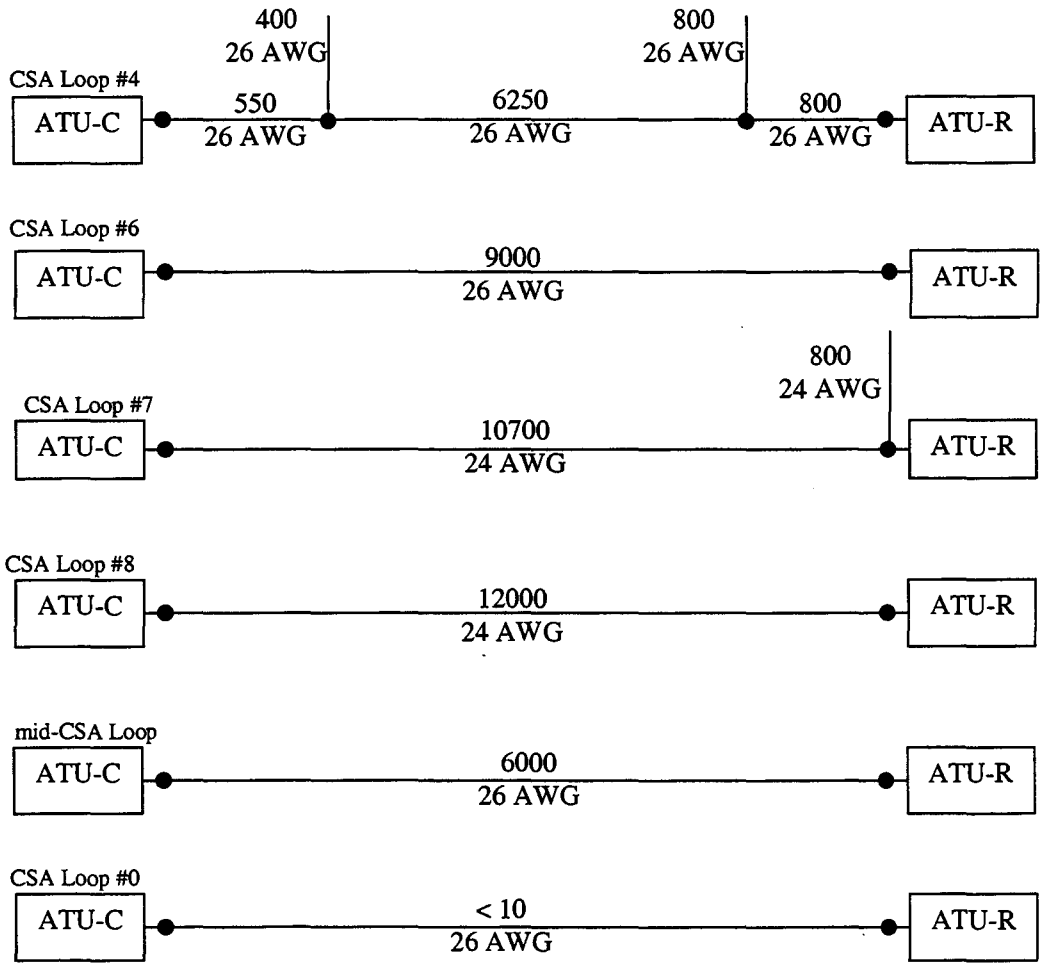

Figure 5.2 ADSL CSA Test Loops (Note: Lengths are in Feet, AWG=American Wire Gauge)

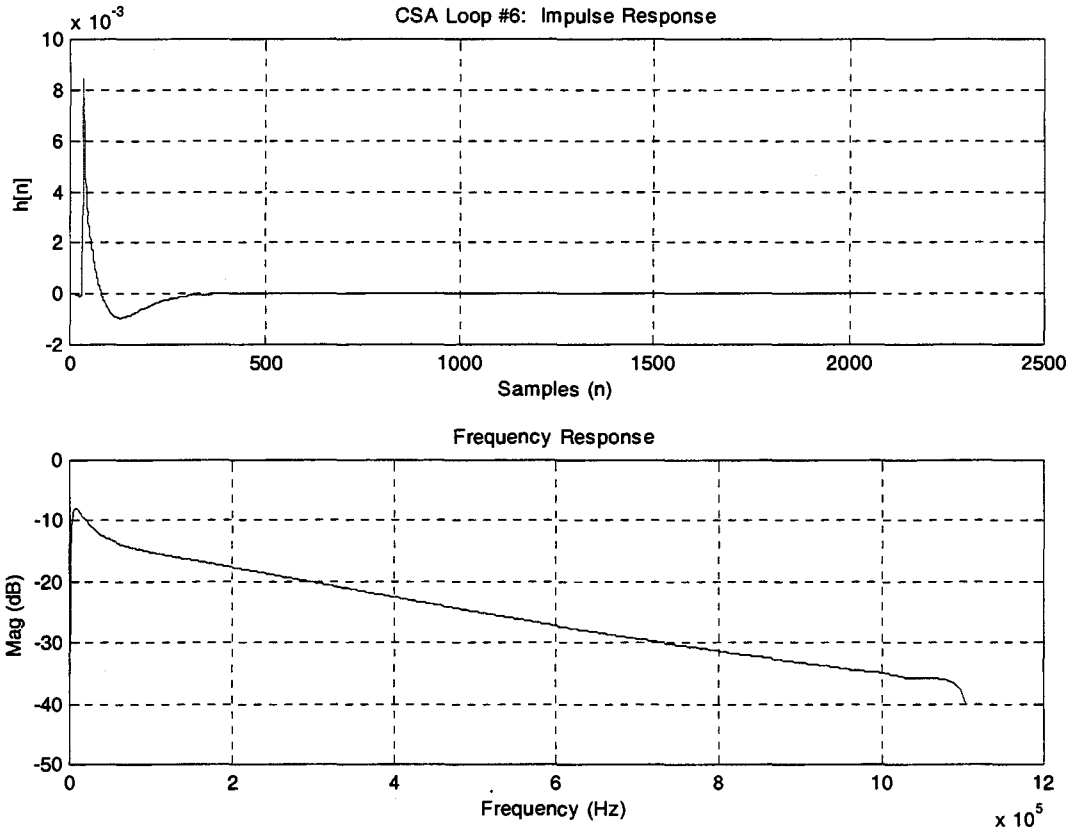

Figure 5.3 CSA Loop #6 Channel Impulse and Frequency Response

5.1.2 ADSL Noise Modeling

There are two types of noise considered in the ADSL simulation:

1. Crosstalk noise
2. Electronics noise

Crosstalk noise is coupled from adjacent wire pairs in the cable bundle and is the dominant noise impairment in CSA and RRD loops. This noise is modeled as

Gaussian and is generated by exciting the appropriate coupling filter by a white Gaussian noise with power of 10mW (10 dBm). The coupling filter is based on 2 types of crosstalk:

1. Near-end crosstalk (NEXT)
2. Far-end crosstalk (FEXT)

NEXT represents a crosstalk of a local transmitter into a local receiver and can be modeled with a coupling function of the form [17],

$$|H_{NEXT}(f)|^2 = K_{NEXT} f^{\frac{3}{2}}$$

where f is the frequency in Hz, and K_{NEXT} is a constant depending on the number of crosstalkers. The crosstalkers range from adjacent T1 carriers to basic-rate ISDN and other xDSL services. The value of K_{NEXT} ranges from 10^{-15} for the fewest crosstalkers to 10^{-13} for the basic-rate ISDN service. Simulations here are performed assuming the worst-case scenario of 49 crosstalkers all due to the ISDN service, where

$$K_{NEXT} = 10^{-13}.$$

FEXT is a crosstalk of a local transmitter into a remote receiver, and is considered negligible in the presence of NEXT and will thus not be included in the simulations.

The other simulated noise is the electronics noise. This includes quantization noise in the analog-to-digital converters (ADC) and thermal noise in the analog portion of the transmitter and receiver. The electronics noise is modeled as an AWGN with power of –30 dBm across the two-sided spectral bandwidth, from –1.104 to 1.104 MHz, for the simulations.

5.2 Simulation Results

In this section the results of the algorithm proposed in section 4 will be applied for equalization of the DMT in an ADSL environment. The simulations are performed using the CSA loop 6, shown in Figure 5.3, sampled at 1.104 MHz. Unless specified, the transmit power is set such that the matched filter bound, MFB,

$$MFB = \frac{\|h\|^2 \sigma_x^2}{\sigma_n^2}$$

of 15 dB is achieved at the receiver to simulate the matched filters used in the transmitter and receiver. To evaluate the performance of the algorithm, the ratio of the signal power to the mean-square error (MSE) is computed,

$$SNR = \frac{\sigma_x^2}{E[|e(n)|^2]}$$

and compared against the optimum solution (MMSE-UEC) derived in section 3.

First, to show the effectiveness of the TEQ, and thus the proposed algorithm, Figure 5.4 shows a comparison of the equalized channel output, the TIR convolved with the given channel ($\boldsymbol{w}_{opt}$*$\boldsymbol{h}$), to that of the TIR $(\hat{\boldsymbol{b}})$. As the figure shows, the algorithm has provided a TEQ that satisfies the need for the long channel impulse response to be constrained to the much shorter length TIR. The difference is due to the residual error.

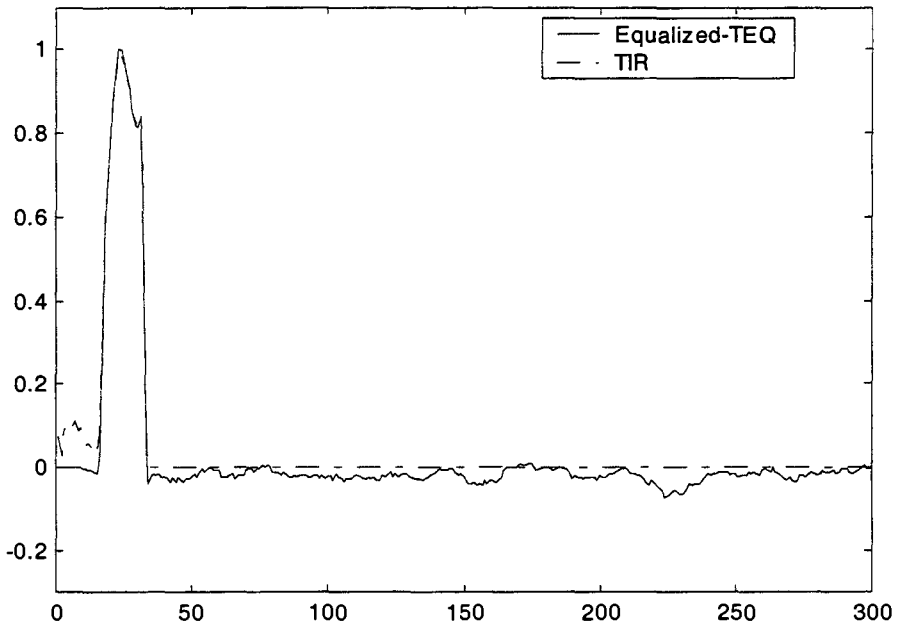

Figure 5.4 Combined Channel-TEQ and TIR Response

Next, in Figure 5.5, the value of the near-end crosstalk coefficient is changed from 10^{-15}-10^{-13} to simulate varying kinds and numbers of crosstalkers. From the plot it can be seen that the performance of the algorithm is constant over the range of K_{NEXT}, and thus the interfering crosstalkers has little effect on the algorithm, verifying that the proposed solution is robust in the presence of crosstalk noise.

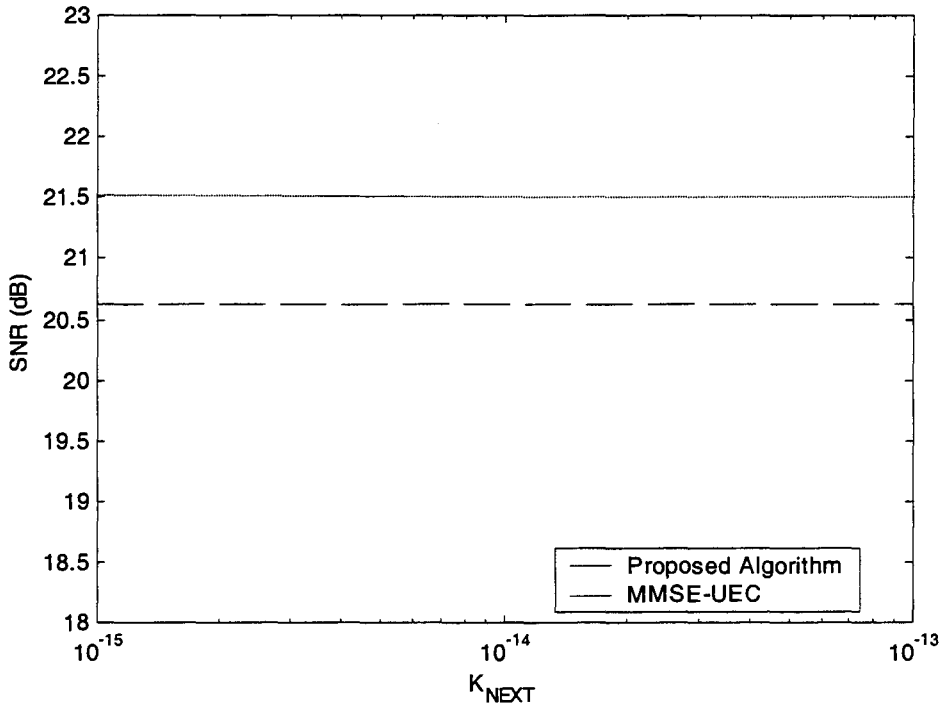

Figure 5.5 Performance Measure as a Function of K_{NEXT}

Finally, in Figure 5.6, the MFB is varied to simulate increasing the transmit power. It can be seen that the SNR increases linearly with the transmit power. This is a desirable feature since an increase in transmit power would result in a higher output SNR. Also the RLS-POCS solution consistently performs .9 dB below the optimal solution for the expected operating range.

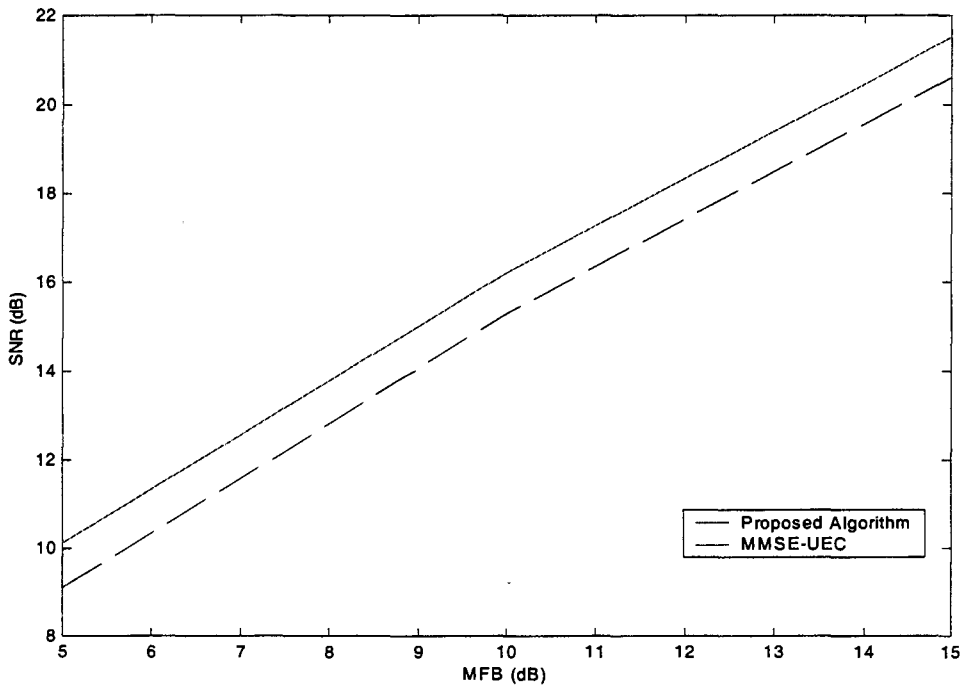

Figure 5.6 Performance Measure as a Function of MFB

As seen in Figures 5.5-5.6, the proposed algorithm has provided a good solution that provides SNR performance within at least .9 dB of the optimal. In these simulations CSA loop 6 was used to provide the worst-case scenario among the CSA loops. As such, use of the other loops will provide an equivalent or slightly better results as was verified through similar simulations.

5.3 Convergence and Complexity Analysis

As stated earlier the LMS algorithm suffers from slow and uncertain convergence. In this section the convergence of the proposed algorithm will be shown and compared with that of the LMS. The tradeoff between convergence rate and final convergence will then be explored through a complexity analysis.

5.3.1 Convergence Analysis

As seen in [4] the convergence rate of the LMS algorithm is very slow. Even after 10,000 iterations the mean square error is still 3 dB away from the MMSE-UEC value. The RLS algorithms are generally known to converge to a solution at least an order faster than the LMS. Thus, the RLS will generally converge to a solution in 2M iterations, where M is the length of the transversal filter [11]. The POCS algorithm on the other hand will converge in a single iteration since the minimum distance of $\left\| \boldsymbol{b}_{opt} - \hat{\boldsymbol{b}} \right\|$ is $\hat{\boldsymbol{b}}$ orthogonal to $\boldsymbol{b}_{opt}$ [14]. Thus the overall convergence rate of the algorithm is due mostly in part to the RLS algorithm which should be seen in the results.

The results of the convergence rate of the RLS-POCS algorithm is shown in Figure 5.7, which represents a sample learning curve for the case when $K_{NEXT}=10^{-13}$ and the SNR=15 dB. From the figure it can be seen that the convergence takes

approximately 1070 iterations, with a residual MSE of only about .8 dB. Since the length of the TEQ is 512, we would expect convergence in approximately 1024 iterations.

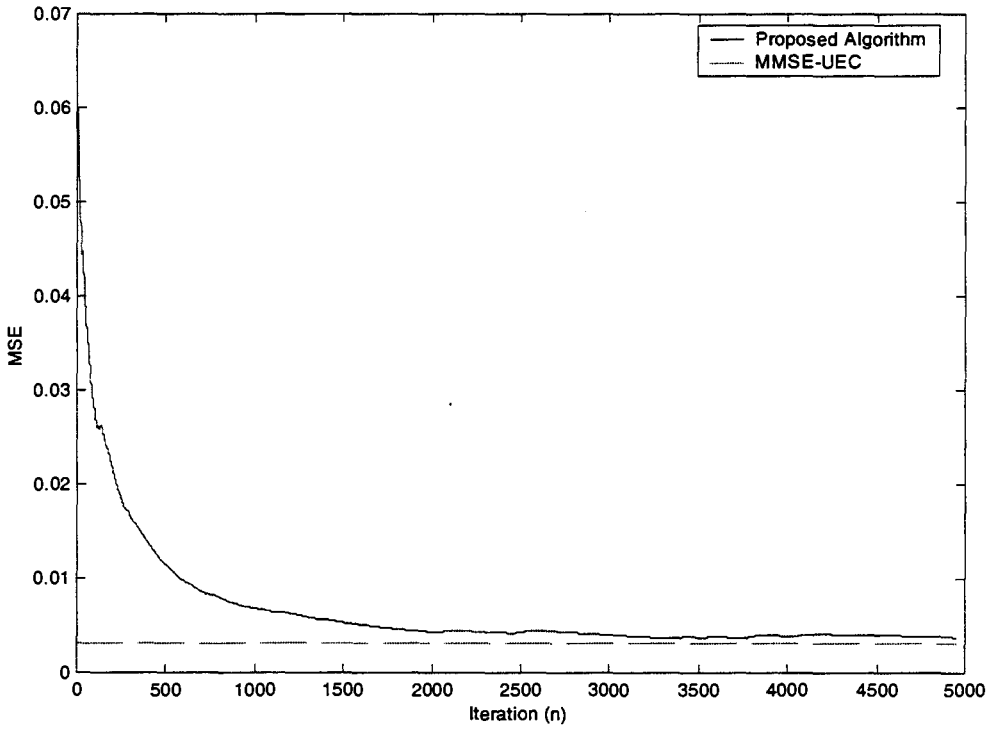

Figure 5.7 Proposed Algorithm Learning Curve

5.3.2 Complexity Analysis

As shown in the previous section the proposed adaption algorithm has a much faster convergence rate, as well as a much lower residual MSE than that achieved using the LMS. This performance increase does come at the cost of higher complexity. Table 5.1 shows the computational requirements for each step of the algorithm shown in section 4.2.3 where the variable N_f is the length of the TEQ.

Calculate Optimal TEQ:

Eqtn.	Calculation	Multiply/Divide	Add/Subtract
4.12	$e(n) = \boldsymbol{x}^T(n)\boldsymbol{b}(n-1) - \boldsymbol{y}^T(n)\boldsymbol{w}(n-1)$	$2N_f$	$2N_f - 1$
4.13	$\mu(n) = \boldsymbol{y}^T(n)R_{yy}^{-1}(n-1)\boldsymbol{y}(n)$	$N_f^2 + N_f$	$N_f^2 - 1$
4.14	$\boldsymbol{g}(n) = \dfrac{R_{yy}^{-1}(n-1)\boldsymbol{y}(n)}{\lambda + \mu(n)}$	N_f	1
4.15	$\boldsymbol{w}_{opt}(n) = \boldsymbol{w}_{opt}(n-1) + \boldsymbol{g}(n)e(n)$	N_f	N_f
4.16	$R_{yy}^{-1}(n) = \dfrac{1}{\lambda}\left[R_{yy}^{-1}(n-1) - \boldsymbol{g}(n)\boldsymbol{y}^T(n)R_{yy}^{-1}(n-1)\right]$	$3N_f^2 + 1$	$2N_f^2 - N_f$
	Total:	$4N_f^2 + 5N_f + 1$	$3N_f^2 + 2N_f - 1$

Calculate Optimal TIR:

Eqtn.	Calculation	Multiply/Divide	Add/Subtract
4.22	$\kappa(n) = \kappa^T(n)R_{xx}^{-1}(n-1)\boldsymbol{x}(n)$	$N_f^2 + N_f$	$N_f^2 - 1$
4.23	$\boldsymbol{gg}(n) = \dfrac{R_{xx}^{-1}(n-1)\boldsymbol{x}(n)}{1 + \kappa(n)}$	N_f	1
4.24	$\hat{e}(n) = \boldsymbol{x}^T(n)\boldsymbol{b}(n-1) - \boldsymbol{y}^T(n)\boldsymbol{w}_{opt}(n)$	N_f	$N_f - 1$
4.25	$\boldsymbol{b}_{opt}(n) = \boldsymbol{b}(n-1) + \boldsymbol{gg}(n)\hat{e}(n)$	N_f	N_f
4.26	$R_{xx}^{-1}(n) = R_{xx}^{-1}(n-1) - \boldsymbol{gg}(n)\boldsymbol{x}^T(n)R_{xx}^{-1}(n-1)$	$2N_f^2$	$2N_f^2 - N_f$
	Total:	$3N_f^2 + 4N_f$	$3N_f^2 + N_f - 1$

Project Optimal TIR:

Eqtn.	Calculation	Multiply/Divide	Add/Subtract
4.30	$\hat{\boldsymbol{b}} = \begin{cases} \boldsymbol{b}_{opt} & \text{if } \boldsymbol{b}_{opt} \in C_1 \\ \boldsymbol{b}_{opt_{Nbx1}} & \text{if } \boldsymbol{b}_{opt} \notin C_1 \end{cases}$	0	0
	Total Operations:	$7N_f^2 + 9N_f + 1$	$6N_f^2 + 3N_f - 2$

Computational Complexity: $O\left(13N_f^2 + 12N_f - 1\right)$

TABLE 5.1 Computational Complexity Calculations of RLS-POCS Algorithm

Thus from Table 5.1 it can be seen that the required operations per iteration is, $O(13N_f^2 + 12N_f - 1)$. In contrast, performing the direct matrix inversion (3.3) would require on the order of $O(3N_f^3)$ to solve for both the optimum TEQ and TIR, noticing the cubic polynomial. The computationally efficient LMS on the other hand only requires $O(3N_f - 1)$, from which convergence is not guaranteed, and the exhaustive search procedure was still required to find the optimum delay. As shown in [4] even after 10,000 iterations the converged solution of the LMS algorithm is still more than 3 dB away from the optimal solution. At the cost of complexity, the proposed algorithm can provide an overall better converged solution in far fewer iterations, thus reducing the required training session time.

A quick note on the complexity requirements in Table 5.1. Matlab calculates $2N_f$ floating-point operations (flops) for every N_f length vector multiplication, in particular Matlab counts N_f additions instead of the customary N_f-1, resulting in 1 extra flop for every vector multiplication. This is in contrast to the $2N_f$-1 flops calculated in Table 5.1, which thus needs to be taken into account to get equivalent results from Matlab.

6. CONCLUSION

6.1 Summary of Results

In this thesis a new algorithm was proposed to provide the partial-equalization needed to shorten the channel impulse response on an ADSL line. The algorithm utilized the RLS error minimization techniques as well as the POCS optimization procedure to provide the solution, and is thus called the RLS-POCS algorithm. It was shown that the new algorithm could provide a much better convergence rate, 1070 iterations versus the 10,000+ required for the LMS. It was also shown that the new algorithm had a much lower residual MSE of less than .9 dB for the worst case scenario, in contrast to the 3 dB of the LMS. It was also shown that the required computational complexity of the proposed algorithm was more on a per iteration basis, but the required time to convergence was far less and far superior to that of the LMS.

6.2 Further Research

Employing the Kalman RLS algorithm to determine the TEQ could further reduce the required computational complexity of the RLS algorithm. Use of the Kalman RLS could result in an overall reduction in computational complexity of 45%. Also, the solution chosen by the method of POCS could possibly yield a better

solution by employing a relaxed projector. In this method the projection operator isn't constrained to being on the surface of the constraint set, but allowed to project to within the set. This could possibly yield a better solution, but it would also require a reevaluation of the constraint set to guarantee that the trivial solution was not chosen as the solution. It would be interesting to see how employing these changes would improve the performance of the ADSL system.

BIBLIOGRAPHY

1. J. Chow, J. Cioffi, and J. Bingham, "Equalizer Training Algorithms for Multicarrier Modulation Systems," *Int. Conf. Commun., Geneva*, May 1993, pp. 761-765.

2. J. Chow and J. Cioffi, "A Cost-Effective Maximum Likelihood Receiver for Multicarrier Systems," *Int. Conf. Commun.*, Chicago, June 1992, pp. 948-952.

3. N. Lashkarian and S. Kiaei, "Fast Algorithm for Finite-Length MMSE Equalizers With Application to Discrete Multitone systems," *IEEE International Conference on Acoustics, Speech and Signal Processing*, Phoenix, AZ April 1999, pp.

4. I. Lee and J. Cioffi, "A Fast Computation Algorithm for the Decision Feedback Equalizer," *IEEE Transactions on Communications*, vol. 43, No. 11., pp. 2742-2749, Nov. 1995.

5. *Asymmetric Digital Subscriber Line (ADSL) Metallic Interface*, ANSI Standard T.413-1995, ANSI, New York.

6. J. Cioffi, G.P. Dudevoir, M. Eyuboglu, and G. Forney Jr., "MMSE Decision-Feedback Equalizers and Coding-Part I: Equalization Results," *IEEE Trans., Commun.*, vol. 43, No. 10, pp. 2582-2594, Oct. 1995.

7. S. Qureshi, "Adaptive Equalization," *IEEE Proc. of the IEEE*, vol. 73, No. 9 pp. 1349-1387, Sept. 1985.

8. N. Al-Dhahir and J. Cioffi, "Efficiently Computed Reduced-Parameter Input-Aided MMSE Equalizers for ML Detection: A Unified Approach," *IEEE Trans. on Info. Theory*, vol. 42, No. 3, pp. 903-915, May 1996.

9. N. Lashkarian and S. Kiaei, "Optimum Equalization of Multicarrier Systems via Projection Onto Convex Set,"

10. N. Al-Dhahir and J. Cioffi, "A Bandwidth-Optimized Reduced-Complexity Equalized Multicarrier Transceiver," *IEEE Trans. on Comm.*, vol. 45, No. 8, pp 948-956, Aug. 1997.

11. S. Haykin, "Adaptive Filter Theory: Third Edition," Prentice Hall, 1996.

12. S. T. Alexander, "Adaptive Signal Processing," Springer-Verlag, 1986.

13. E. Kreyszig, "Advanced Engineering Mathematics: Seventh Edition," John Wiley & Sons, 1993.

14. H, Stark and Yang, "Vector Space Projections," John Wiley & Sons, 1998.

15. T. Inoue, "Modified Conjugate Gradient Method for ADSL Echo Cancellation," Masters Thesis, Oregon State University, Corvallis, OR, 1998.

16. *Standards Project for Interfaces Relating to Carrier to Customer Connection of Asymmetrical Digital Subscriber Line (ADSL) Equipment,"* ANSI Standard T.413-1998 Issue 2, ANSI, Texas.

17. D. Messerschmitt, "Design Issues in the ISDN U-Interface Transceiver," *IEEE Journ. Select. Areas Comm.,* vol SAC-4, No. 8, pp. 1281-1293, Nov. 1986.

18. I. Lee, J. Chow, J. Cioffi, "Performance Evaluation of a Fast Computation Algorithm for the DMT in High-Speed Subscriber Loop," *IEEE Journ. Select. Areas Comm.,* vol 13, No. 9, pp. 1564-1570.